Defining the relationship between a baculoviral sulfhydryl oxidase and a potential accessory protein

by

Adam Joseph Schieferecke

B.S., Kansas State University, 2017

A THESIS

submitted in partial fulfillment of the requirements for the degree

MASTER OF SCIENCE

Division of Biology
College of Arts and Sciences

KANSAS STATE UNIVERSITY
Manhattan, Kansas

2018

Approved by:

Major Professor
Dr. Ana Lorena Passarelli

Copyright

Abstract

Baculoviruses are a large, diverse, and an ecologically-important group of entomopathogens. The *ac78* gene of the prototype baculovirus, Autographa californica multiple nucleopolyhedrovirus (AcMNPV), is one of the 38 genes conserved among all baculoviruses sequenced to date. Previous studies show that Ac78 is essential for optimal production of occlusion-derived virions (ODVs) and budded virions (BVs), which are two virion types produced during baculovirus infection. However, the biochemical mechanism by which Ac78 is involved in these processes remains unknown. The AcMNPV sulfhydryl oxidase *ac92* is a conserved gene, and its product, Ac92, is ODV and BV envelope-associated. Recently, the Ac78 and Ac92 homologs in Helicoverpa armigera nucleopolyhedrovirus (HearNPV) were reported to interact and co-localize to the site of BV and ODV formation. To investigate the relationship between Ac78 and Ac92, we determined their localization in the presence and absence of AcMNPV infection, performed co-immunoprecipitations to assess interaction relationships, and provided an updated report of Ac78 and Ac92 homology with other proteins. We concluded that in the absence of viral infection, Ac78 and Ac92 localized perinuclearly in the cytoplasm and that localization of Ac92 was not affected by Ac78. During AcMNPV infection, Ac78 and Ac92 co-localized within the nucleus and surrounding virus replication and assembly sites (ring zone). Co-immunoprecipitation experiments showed that at least two differentially-tagged Ac78 proteins were part of a complex in the presence of other AcMNPV proteins. Ac78 did not associate with Ac92 during AcMNPV infection. Our characterization of the relationship between Ac78 and the AcMNPV sulfhydryl oxidase is a preliminary step in a broader effort to elucidate important biochemical pathways underlying the poorly described structural changes in capsid proteins and other proteins involved in virion stability, folding, and infectivity.

In a separate project, the same approach was applied in a different virus system to determine the relationship between the small accessory protein C and the measles virus (MeV) replication complex. Co-immunoprecipitation experiments showed that during MeV infection, C associated with large protein (L) and phosphoprotein (P), which comprise the MeV replication complex, and nucleoprotein (N), which encapsidates the RNA genome. Expression constructs for full-length MeV L were generated, and L was successfully expressed following transfection. Subsequent co-immunoprecipitation experiments showed that C did not precipitate with L, P, nor N when transfected in isolation from MeV infection, indicating that another factor resulting from MeV infection is necessary for the association of C with the MeV replication complex. The results of this investigation are an important step in elucidating a biochemical mechanism underlying the function of C as a quality control factor in MeV replication. MeV has been attenuated and is a highly effective vaccine against pathogenic MeV and an active subject of clinical research as an oncolytic agent for treating a number of human cancers.

Taken together, the investigations of Ac78 and C and their respective relationships with the AcMNPV sulfhydryl oxidase and the MeV replication complex adds knowledge of biochemical mechanisms underlying the important functions of small accessory proteins containing less than 200 amino acids as mediators in viral replication processes of two different viral systems.

Table of contents

List of figures

List of tables

Acknowledgements

I would like to particularly thank my research mentor, Dr. A. Lorena Passarelli, for her excellent guidance and support as a personal mentor during the first three years of the BS/MS program and as my primary research supervisor during the last two years of the program. She has been an excellent teacher and helped me to mature into a skilled and independent researcher.

Dr. Dan Boyle of Kansas State University deserves particular recognition, as he provided technical support with the confocal microscopy techniques used to determine localization of Ac78 and Ac92 in the presence and absence of viral infection.

Dr. Roberto Cattaneo, Principle Investigator, and Dr. Christian Pfaller, Postdoctoral Researcher, of the Virology and Gene Therapy Track in the Department of Molecular Medicine at Mayo Clinic are acknowledged for hosting me as a summer student and contributing intellectual content to the work presented in Chapter 4 of this master's thesis.

I wish to thank past research supervisors from the undergraduate portion of my studies, specifically Dr. Greg Ragland and Dr. Stefan Rothenburg. Their mentorship and guidance early in my undergraduate studies provided the knowledge necessary to successfully complete this master's thesis work. Two former graduate students of the laboratory of Dr. Stefan Rothenburg, Drs. Sherry Haller and Chen Peng, were patient teachers of the fundamental molecular biology techniques that served as my foundational skill-set for being able to complete this master's thesis work.

Finally, I wish to thank my family, who motivate me to generate human knowledge of the natural world and whose support makes my pursuits possible.

Dedication

This master's thesis work is dedicated to my son, Addis, and wife, Alexa, who are the driving source of motivation for every scientific question I pursue.

Preface

This master's thesis report, "Defining a baculoviral oxidoreductase pathway", adds to our understanding of the mechanism by which the small, 12.5 kDa, baculoviral-encoded protein, Ac78, is involved in the production of virions. This report has been written to partially fulfill the graduation requirements of the MS program in Biology at Kansas State University (KSU). I was engaged in this research from October 2016 – July 2018 as part of the joint BS/MS program in the Division of Biology and in writing this thesis report from May 2018 – July 2018.

Work that I performed early in the undergraduate portion of my studies led to my interest in the work presented in this master's thesis report. I began my undergraduate research experience in the lab of Dr. Stefan Rothenburg immediately upon entering KSU as a first-year undergraduate student in September 2013. The Rothenburg lab studies evolutionary arms races between viruses and its hosts using poxviruses as a model. I was influenced by a paper that shows that myxoma virus (MYXV), a poxvirus and natural rabbit pathogen that cannot establish an active infection in humans, exhibits significant oncolytic activities in some human cancers (Lun, et al., 2005). Not all human cancers, however, are sensitive to the oncolytic effects of MYXV. Our lab hypothesized that the lack of inhibition of the antiviral human protein kinase R (PKR) by MYXV's endogenous inhibitor gene of PKR, M156R, could explain why some cancers that exhibit high PKR activity are resistant to oncolysis by MYXV. The question that I focused my first undergraduate research project to address was: does the incorporation of more effective inhibitors of human PKR in MYXV lead to enhanced oncolytic activities in cells that express high levels of PKR? To answer this question, I assisted a graduate student in the lab in generating two recombinant MYXVs by replacing M156R with its orthologs from racoon or deer poxvirus, which exhibit intermediate and strong levels of human PKR inhibition, respectively. I

tested whether recombinant MYXVs exhibit increased replication levels compared to wild type MYXV (wt-MYXV) in four different human cancer cell lines. I subsequently optimized experiments to systematically test whether there is a correlation between PKR expression and MYXV sensitivity. The relocation of the Rothenburg lab to the University of California, Davis cut my involvement in this project short at the end of my third year at KSU. However, this project is being continued by current students.

Studying MYXV led to my concurrent interest in squirrel fibroma virus (SQFV), a previously uncharacterized poxvirus that is closely related to MYXV. I worked on a collaborative investigation in which I assisted in characterizing the host-range of SQFV, determining the phylogenetic relatedness of SQFV with other poxvirus species, and annotating the SQFV genome. Genome annotation uncovered numerous interesting features, including that SQFV contains the longest inverted terminal repeat sequence (19.5 kb) of any known poxvirus and evidence for a recombination event that occurred between an ancestral virus and a distantly-related poxvirus. A manuscript for which I am a co-author is currently being drafted with Rothenberg lab members in collaboration with the laboratory of Nels Elde at the University of Utah.

Characterizing the SQFV genome led me to seek a broader skillset in genomics in order to gain evolutionary insights. I completed a vigorous 14-week investigation in the arthropod genomics lab of Dr. Greg Ragland. My first project was a collaborative effort which explored the question of how genes are differentially expressed during dormancy developmental progression in two speciating populations of the agricultural apple maggot pest *Rhagoletis pomonella*. I identified and edited candidate genes of interest, presented a poster at two national scientific conferences, and assisted with writing a manuscript published in *Journal of Experimental Biology* of which I

am a co-author (Meyers et al., 2016). The results of this project showed that differences in the transcriptome contributed to adaptive differences in climate tolerance and food source among the two speciating populations. I also contributed to answering the question: what is the phenotypic response to overwintering of another invasive agricultural pest, the spotted winged fruit fly, *Drosophilia suzukii?* We found that both low temperature and short photoperiod resulted in reduced level of development. A manuscript for which I am co-author was published in *Journal of Environmental Entomology* (Everman et al., 2018).

In addition to learning genetic and genomic approaches, I wanted to add to my virologist toolbox by gaining proficiency in biochemical approaches. My 10-week fellowship in the laboratory of Dr. Roberto Cattaneo provided this opportunity. My project aimed to determine the mechanism by which the measles virus (MeV)-encoded C protein interacts with the MeV replication complex. Such knowledge is important because the attenuated vaccine-strain MeV is a promising and active subject of oncolytic viral therapy research and numerous members of the *Mononegavirales* order to which MeV belongs are significant human pathogens. This work was performed during the undergraduate portion of the joint BS/MS program and uses a highly related approach to that of my master's thesis work performed in the laboratory of my major professor, Dr. A. Lorena Passarelli. Thus, the results of my investigation of the interaction between C protein and MeV polymerase has been included as the third chapter in my master's thesis report with permission and input from Drs. Roberto Cattaneo and Christian Pfaller of the Department of Molecular Medicine at Mayo Clinic.

My work in the laboratory of Dr. A. Lorena Passarelli, which began at the start of my fourth year at KSU, was a continuation of my study of viral protein interactions. This work, which is the subject of the first two chapters of this thesis report, investigates the relationship between a

highly conserved baculoviral protein, Ac78, and the baculoviral sulfhydryl oxidase, Ac92. I am excited to share this work with the scientific community and the general public. Engaging in this work has developed my competencies as an independent researcher, which will be applied in years to come.

I hope you enjoy reading,

Adam J. Schieferecke

Manhattan, KS, May 20, 2018

References - preface

Everman ER, Freda PJ, Brown M, Schieferecke AJ, Ragland, GJ, and Morgan TJ. (2018). Ovary development and cold tolerance of the invasive pest Drosophila suzukii Matsumura in the central plains of Kansas, United States. *J. Environmental Entomology*. Doi 10.5061/dryad.kj

Lun X, Yang W, Alain T, Shi ZQ, Muzik H, Barrett JW, McFadden G, Bell J, Hamilton, MG, Senger DL, Forsyth PA. (2005). Myxoma virus is a novel oncolytic virus with significant antitumore activity against experimental human gliomas. *Cancer Res. 1;65*(21), 9982-9990. Doi 10.1158/0008-5472

Meyers PJ, Powell TH, Walden KK, Schieferecke AJ, Feder JL, Hahn DA, Robertson HM, Berlocher SH, Ragland GJ. (2016). Divergence of diapause transcriptome in apple maggot flies: winter regulation and post-winter transcriptional repression. *J. Exp Biol. 1;219*(17), 2613-22. Doi 10.1242/140566

Chapter 1 - literature review

1.1 Baculoviruses

Baculoviridae is a large, diverse, and an ecologically-important family of entomopathogens that naturally infect the larvae of over 600 species of lepidopteran, dipteran, and hymenopteran insects (Martignoni, 1981). Baculoviruses are organized into four genera: alphabaculoviruses, betabaculoviruses, deltabaculoviruses, and gammabaculoviruses. The four genera are demarcated by distinguishing features including phylogeny based on DNA sequences from various regions of the genome, predicted protein sequence similarities, DNA restriction profiles, and host range and specificity. Gammabaculoviruses infect the larvae of Hymenoptera, deltabaculoviruses infect the larvae of Diptera, and alphabaculoviruses and betabaculoviruses infect the larvae of Lepidoptera (ICTV, 2017). Alpha-, gamma-, and deltabaculoviruses are referred to as nucleopolyhedroviruses (NPVs), whereas the betabaculoviruses are refered to as granuloviruses reflecting differences in the occlusion body morphology and protein composition. The baculoviral genome is composed of circular, double-stranded DNA (dsDNA) that ranges from 80 to 180 kilobase pairs (kbp) in length. The name “baculovirus” is derived from the Latin word *baculum* and refers to the rod-shaped nucleocapsids which encapsidate the baculoviral genome (Rohrmann, 2011). Alpha-, beta- and gamma-baculoviruses produce two different types of virions, which possess identical genetic information and nucleocapsid structures but are produced at different time points during the replication cycle and possess distinct envelope compositions according with different roles in the infection cycle. One type of virion, budded virus (BV), is used to spread the infection from cell-to-cell within the host. The other type of virion, occlusion-derived virus (ODV), is used to spread the infection from host-to-host through the outside environment. NPVs in which the

envelope of the ODV contains only one nucleocapsid are designated as a single NPV (SNPVs), and NPVs in which the ODV envelope contains two or more nucleocapsids are designated multiple NPVs (MNPVs).

The baculovirus replication cycle begins when a larva ingests occlusion bodies, which dissolve in the alkaline environment of the midgut lumen and release ODV. The released ODV particles subsequently infect mature columnar epithelial cells, initiating primary infection in the midgut. Inside the cells, viral replication and virion assembly occurs in the nucleus. BVs are formed when newly assembled nucleocapsids egress from the nucleus, migrate through the cytoplasm, and bud from the plasma membrane. These progeny BVs then establish systemic infection throughout the rest of the host. Late during infection, ODV is produced and accumulated into occlusion bodies, which are crystalline matrixes composed of the polyhedrin protein in NPVs. Upon cell death, aggregated ODV inside occlusion bodies are released back into the environment, in which they remain infectious until a new host ingests them (Rohrmann, 2011).

The study of baculoviruses has immense ecological, agricultural, economic, and scientific importance. Baculoviruses play a critical ecological role in many ecosystems by naturally regulating insect populations (Podgwaite, et al., 1981; Bonsall, 2004; Myers & Cory, 2015). This observation from nature led baculoviruses to be harnessed as biological pesticides to protect agricultural crops. Baculoviruses have proven success at managing a number of infamous pest populations such as the larvae of *Galleria mellonella*, *Phthorimaea operculella*, *Spodoptera littoralis*, which destroy honey bee hives, potatoes, and cotton, respectively. Additionally, there are several extant examples of baculoviruses being successfully implemented in the applied control of Lepidoptera and Hymenoptera forest pests (Moscardi, 1999; Summers, 2006; Beek & Davis, 2016). Presently, there are thirteen NPV pesticide formulations against Lepidoptera and

Coleoptera listed as approved for commercial use in the United States (Kalha et al., 2014; EPA, 2016). While a large need exists, widespread use of NPV-based pesticides has been limited by large-scale production challenges and efficacy of killing target pests in the field. For example, ensuring the baculovirus suspension is delivered in a way that ensures the insects ingest the product and that the replication cycle of the baculovirus is faster than the reproduction cycle of the insect are particularly critical challenges to overcome when developing commercial baculoviral pesticide products. For this reason, acquiring increased understand of the underlying molecular mechanisms of baculoviral replication processes continues to be important. Additionally, baculoviruses are harnessed as protein expression systems in insect and mammalian cell systems. (Chen et al., 2011; Kost et al., 2005; Possee, 1997; Condreay, 2007). Such baculoviral protein expression systems are sold commercially by companies such as Thermo Fischer (Thermo Fischer, 2018). Further, baculoviruses have been used as effective models in the study of gene regulatory networks and whole genome evolution and have significantly expanded our knowledge of apoptosis (Herniou et al., 2001; Oliveira et al., 2013).

Much of the current knowledge of MNPVs was acquired through the study of the prototype baculovirus AcMNPV originally isolated from the alfalfa looper moth *Autographa californica* (Vail et al., 1971). The naming of AcMNPV after the host species from which it was first isolated set precedent for the naming system of future baculoviruses. However, it later became known that AcMNPV infects many different Lepidopteran species beyond *Autographa californica* (Taha et al., 1995; Miller & Lu, 1997). The AcMNPV genome is approximately 134 kbp long and contains 154 predicted open reading frames (ORFs) (Maghodia et al., 2014), including the 38 “core genes” conserved in the over 80 baculovirus genomes completely sequenced to date (Garavaglia et al., 2012; Javed et al., 2017). Because of their conservation,

each of these core genes is likely to play an essential role in the baculovirus replication cycle. Two of these core genes, Ac92 and Ac78, are discussed in greater detail in sections 1.4 and 1.5, respectively.

1.2 Disulfide bonds and sulfhydryl oxidation

The disulfide bond is a prevalent type of covalent linkage between the thiol (SH) groups of two cysteine residues in proteins. Disulfide bonds are essential components of protein structures by providing structural covalent linkages between amino acid residues and by participating in biologically important oxidation-reduction (redox) reactions. Disulfide bonds exhibiting redox activity comprise intramolecular protein disulfides. These disulfide bonds play extremely important biological roles in activating and deactivating proteins and altering cellular localization of proteins based on redox changes in the environment. Disulfide bonds are formed when the nucleophilic sulfur anion belonging to the side chain of one cysteine residue attacks the side chain of the other interacting cysteine. This nucleophilic attack releases two electrons that are transferred to another molecule, such as a flavin adenine dinucleotide (FAD) cofactor (Sevier et al., 2012). Because cysteine is the only amino acid that can participate in this reaction, its presence in proteins has immense functional consequences and has been found to be highly conserved throughout evolution (Jones et al., 1992; Gonnet et al., 1992). Cysteine residues are found in every sequenced life form to date. Approximately half of all cysteine residues participate in disulfide bonds (Rubinstein & Fiser, 2008), and these disulfide-bonded cysteines are the most conserved amino acids in proteins (Wong et al., 2010). In order for protein disulfide bond formation to occur, the interacting cysteine pair must be located in close enough physical

proximity to one another and the interaction environment must exhibit oxidizing conditions and a relatively high pH (Bechtel & Weerapana, 2017). Thus, locations in the cell that exhibit oxidizing and pH conditions conducive for disulfide bond formation must exist.

In eukaryotes, the endoplasmic reticulum (ER) exhibits an oxidizing environment conducive to the loss of hydrogens from the sulfur atoms on thiol groups of cysteine residues and the subsequent formation of disulfide bonds with other oxidized cysteine residues. The formation of disulfide bonds in the ER is regulated by oxidoreductases that catalyze the reaction, such as members of the thioredoxin family and members of the protein disulfide isomerase (PDI) family that contain thioredoxin-like domains (Darby & Creighton, 1995; Hatahet et al., 2009; Sevier et al., 2002; Fiege et al., 2011). Disulfide bonds are necessary for proteins to be able to maintain proper conformation under the highly oxidizing conditions commonly found in extracellular environments. Accordingly, disulfide bonds are commonly found in proteins bound for the secretory pathway. Because the cytosol and nucleus are highly reducing environments (Gilbert, 1990) not conducive to the formation of disulfide linkages between cysteines, cytosolic and nuclear proteins in mesophilic organisms rarely contain structural disulfide bonds.

In prokaryotes, disulfide bond formation is carried out in the oxidizing environment of the periplasm (Landeta et al., 2018). As in eukaryotes, disulfide bonds are not commonly found in cytosolic proteins but are common in secreted proteins. As with eukaryotic secretory proteins, prokaryotic secretory proteins require reinforcing covalent bonds in order to withstand the severe oxidizing extracellular environment. Adding disulfide bonds to secreted proteins on their way out of the cell provides this needed structural reinforcement. Disulfide bond formation in the periplasm is catalyzed by an oxidoreductase that belongs to the same thioredoxin superfamily as PDI called DsbA (Bardwell et al., 1991). A growing body of evidence shows the essential roles

of disulfide bonds in the stability of virulence factors of pathogenic bacteria. Consequently, the study of disulfide bonds in prokaryotic systems is currently an active area of research (Landeta et al., 2018)

More recently, it has become known that eukaryotic disulfide bond formation occurs in the mitochondria as well. Mitochondria are derived from bacterial ancestors that permanently became cellular organelles through an endosymbiont event (Embley & Martin, 2006). Mitochondria contain their own genome and encode several proteins that are synthesized in the cytosol and transported back into their respective mitochondrial compartments. Because both the mitochondria and the cytosol are reducing environments of proteins, it was once assumed that the mitochondria did not carry out disulfide bond formation. However, it is now known that numerous proteins located in the mitochondrial intermembrane space (IMS), including the copper chaperon Cox17 involved in the biogenesis pathway of cytochrome oxidase (Glerum et al., 1996) and members of the translocase of the inner membrane (TIM) complex that chaperone hydrophobic proteins (Bauer et al., 2000; Stojanovski et al., 2008), contain disulfide-bonded cysteines. To carry out sulfhydryl oxidation in the mitochondrial intermembrane space (IMS), a folding-trap relay system composed of two essential components is utilized; Mia40 serves as an electron shuttling protein and is subsequently oxidized by the FAD-linked electron acceptor Erv1, which uses FAD to pass the electrons to molecular oxygen. (Deponte & Hell, 2009). It is now known that this system participates in the redox reactions of many different proteins that are present in the IMS (Wrobel et al., 2016).

Redox reactions carried out by PDIs have net reactions that result in the exchange of one disulfide bond for another, whereas redox reactions carried out by sulfhydryl oxidases result in a net production of disulfide bonds. Sulfhydryl oxidases contain a flavin as an essential cofactor

(Argyrou & Blanchard, 2004) and at least one CXXC active site that accepts electrons through the reduction of oxygen into hydrogen peroxide (Hoober & Thorpe, 1999). Members of Plantae, Animalia, and Fungi have been found to contain cellular FAD-linked sulfhydryl oxidases (Fass, 2008). Additionally, sulfhydryl oxidases are present in many of the nucleocytoplasmic large DNA viruses (NCLDVs) (Hakim & Faas, 2010) and every baculovirus sequenced to date (Figure 2.1). Today sulfhydryl oxidases are classified into four major families: endoplasmic reticulum oxidases (Ero), qiescin sulfhydryl oxidases (QSOX), secreted sulfhydryl oxidases of fungi, and Erv.

1.3 Viral sulfhydryl oxidation

Many of the large, complex DNA viruses, including NCLDVs and baculoviruses, encode their own Erv-family-like sulfhydryl oxidases in order to promote disulfide bond formation in the reducing environments of the cytoplasm and/or nucleus. Currently, NCLDVs include the seven taxonomic families *Ascoviridae*, *Asfarviridae, Iridoviridae, Marseilleviridae, Mimiviridae, Phycodnaviridae,* and *Poxviridae* (Gallot-Lavallée & Blanc, 2017). Studies of three molecularly characterized viral sulfhydryl oxidases, vaccinia virus E10R (Senkevich et al., 2000), African swine fever virus (ASFV) pB119L (Rodríguez et al., 2006), and mimivirus R596 (Hakim et al., 2012), have revealed mechanisms by which viruses are able to co-opt processes involved in cellular protein synthesis to successfully carry out their own disulfide bond formation in the highly reducing environment of the cytoplasm.

Vaccinia virus E10R was the first viral sulfhydryl oxidase characterized (Senkevich et al., 2000). The finding that a virus encodes its own functional sulfhydryl oxidase that allows it to control

redox processes in the cytoplasm was a huge discovery. Vaccinia virus is a prototype poxvirus that replicates in the cytoplasm of infected cells. Vaccinia virus sulfhydryl oxidase electron shuttling occurs through the FAD-linked sulfhydryl oxidase E10R forming a stable disulfide bond with the CXXXC motif of the oxidoreductase A2.5L, which then forms a transient disulfide-linked complex with G4L and the subsequent oxidation of structural components of the virion membrane (Senkevich et al., 2000; Senkevich et al., 2002). It is likely that this pathway occurs universally in poxviruses, as the involved proteins are highly conserved among poxviruses as well as several other NCLDVs (Saaranen & Ruddock, 2013).

The ASFV FAD-linked sulfhydryl oxidase pB119L is a late protein required for the assembly of infectious virions and uses a very similar pathway for sulfhydryl oxidation as described for poxviruses. pB119L forms a disulfide interaction with the CXXC motif of the thiol oxidoreductase pA151R, which subsequently forms an interaction with the structural protein pE248R that has homology to vaccinia L1R structural protein (Rodríguez et al., 2006). This study showed that similarities to the mechanisms used by the vaccinia virus sulfhydryl oxidation pathway exist in other viral systems beyond poxviruses.

The characterization of the mimivirus FAD-linked sulfhydryl oxidase R596 uncovered an enormous protein containing a major subunit in addition to a catalytic domain similar to that of other Erv family sulfhydryl oxidases (Hakim et al., 2012). Mimivirus revealed a novel mechanism of sulfhydryl oxidation in which the disulfide relay occurred between subunits within the R596 dimer. The complex structure of R596 has similarities to those of cellular QSOXs in addition to viral Erv family sulfhydryl oxidases; cellular QSOX orthologs contain a thioredoxin fold in a different domain of the same protein as the Erv-family sulfhydryl oxidase active site.

Further, the massive sulfhydryl oxidase gene of mimivirus was shown to be highly conserved among the other sequenced giant viruses (Hakim et al., 2012).

Viral sulfhydryl oxidases play an essential role in the replication cycles of a number of large, complex viruses. Aside from being intrinsically fascinating, the vigorous pursuit to increase understanding of the underlying biochemical functions and mechanisms of viral sulfhydryl oxidases and disulfide bond formation elucidates valuable information that can potentially be targeted in the development of novel antiviral therapies and viral vectors for gene delivery.

1.4 Ac92: the baculoviral sulfhydryl oxidase

The conserved baculoviral gene *ac92* encodes an Erv family FAD-linked sulfhydryl oxidase that is conserved in all known baculoviruses to date (Long et al., 2009; Wu and Passarelli, 2010; Figure 2.1). The functionality of the baculoviral sulfhydryl oxidase may be conserved or partially conserved in some baculoviruses. For example, the Ac92 homolog Tn79 of Trichoplusia ni nucleopolyhedrovirus was able to serve as a partially functional sulfhydryl oxidase when the endogenous *ac92* was knocked out of AcMNPV and replaced with *tn79* (Clem et al., 2014). Ac92 contains a CXXC active site and associated FAD cofactor arrangement that is highly similar to the CXXC site and FAD cofactor arrangement of other Erv family sulfhydryl oxidases widely found in a range of eukaryotic species and NCLDVs (Hakim et al., 2011). However, a majority of the experimentally-derived structure of Ac92 is highly divergent from other Erv family sulfhydryl oxidases (Fass, 2008; Hakim and Fass, 2010; Hakim et al., 2011). For example, Ac92 contains complex structural arrangements in additional domains that are not homologous to any other known protein. Moreover, while cellular Erv family sulfhydryl

oxidases contain an additional CXXC motif flanking the Erv region (Faas, 2007), P33 family sulfhydryl oxidases contain only one CXXC motif.

Ac92 is known to be essential for the formation of infectious BV and multiply enveloped ODV (Nie et al., 2011; Wu and Passarelli, 2010). Viruses with a deletion of in *ac92* exhibit similar phenotypes to viruses in which the two cysteines in the CXXC active site are mutated to alanines (Wu and Passarelli, 2010). The results of these studies confirm the essential function of Ac92 sulfhydryl oxidation in the assembly of mature infectious AcMNPV virions. Although Ac92 sulfhydryl oxidation is essential for the production of ODV and BV, the substrate or substrates targeted by Ac92 during baculovirus infection remain unknown. The non-active site domains of Ac92 are not thought to contain their own thiol redox active protein as in cellular and mimivirus Erv family sulfhydryl oxidases (Hakim et al., 2011). Thus, a different viral or cellular protein with oxidoreductase activity must serve this purpose. Ac92 was first noticed when it was found to interact with human P53 (Prikhod'ko et al., 1999). Ac92 was also shown to interact with the *Spodoptera frugiperda* P53 (SfP53) (Wu et al., 2014). However, this study was unable to identify any functional implications that the Ac92-P53 interaction may have in viral replication processes. In NCLDVs such as poxviruses, the major components of the redox pathway are encoded within the viral genome. It is possible that baculoviruses also evolved to encode all of the major components of their redox pathway within their genome, and that these components are waiting to be characterized. One baculoviral protein was reported to interact with the P33 homolog; the Ac92 homolog in Helicoverpa armigera nucleopolyhedrovirus was shown to interact with the Ac78 homolog (Huang et al., 2014). The authors of this study hypothesized that Ac78 may work in a redox process with Ac92. However, unlike the thiol oxidoreductases that interact with the poxviral sulfhydryl oxidases, Ac78 does not contain a CXXC motif required for

disulfide bond formation. If the baculoviral sulfhydryl oxidase system is similar to the poxvirus system and encodes all components of its redox chain in the genome, then it is likely that the oxidoreductase component responsible for the shuttling of electrons from Ac92 to viral membrane motifs would contain a CXXC motif.

1.5 Ac78: an essential baculoviral accessory protein

The baculoviral gene *ac78* is among the 38 core genes conserved among all sequenced baculoviral species to date (Garavaglia et al., 2014; Javed et al., 2017). The conservation of Ac78 among all known baculovirus species indicates an essential role in the viral replication cycle. Ac78 is associated with the envelope of ODV (Tao et al., 2013; Li et. Al, 2014). When *ac78* was deleted from AcMNPV, viral DNA replication appeared to be unaffected, nucleocapsids were confined to the nucleus, occlusion bodies lacked ODV, and BV and ODV were not produced (Tao et al., 2013) or produced in very low levels (Li et. Al, 2014). A study in which the Ac78 homolog Bm64 in Bombyx mori nucleopolyhedrovirus was disrupted corroborated with the conclusion that Ac78 is essential in baculoviral infection cycle. When Bm64 was knocked out, few infectious BVs were produced, and although ODV and occlusion bodies formed, the ODV could not establish infection in a new host (Chen et al., 2015). An Ac78 homolog was additionally shown to be ODV envelope-associated in a third baculovirus species, HearNPV (Hou et al., 2013). Neither Ac78 nor any of its tested homologs appear to affect viral DNA replication.

While it is clear that Ac78 plays an important function in the AcMNPV replication cycle, the biochemical mechanism by which Ac78 is involved in the production of virions remains

unknown. Ac78 was recently reported to interact with Vps4, the key regulator for recycling the endosomal sorting complex required for transport III (ESCRT-III) (Yue et al., 2017). It had previously been shown that Vps4 is required for optimal infection by AcMNPV. Additionally, Ac78 was recently shown to associate with the N-ethylmaleimide-sensitive factor (NSF). NSF is the key regulator of the soluble NSF attachment protein receptor (SNARE) system, which mediates fusion of transport vesicles with target membranes in cells. Together, these recent findings suggest Ac78 could play a role in baculoviral entry and egress.

Ac78 has been reported to contain a motif that was originally characterized in the baculovirus protein ODV-E66 as an internuclear membrane signaling motif that functions as an N-terminal localization signal of proteins to the intranuclear ring zone and the ODV envelope (Li et al., 2014). An 18-amino acid long hydrophobic sequence within this predicted signaling motif serves as a transmembrane motif, which are conserved as primarily hydrophobic residues in 79 other Ac78 orthologs (Figure 2.2). It has been reported that amino acid residues located in the conserved N-terminal regions (sites 2-25) and C-terminal regions (sites 64-88) are important for the function of Ac78. When the middle lysine of the IPLKL motif was deleted in HearNPV, the function of Ac78 and the interaction with P33 were disrupted. The N-terminal region of Ac78 has homology with C-terminal residues in an oxidoreductase of *Danaus plexippus* (Zhan et al., 2011; Li et al., 2014). Likewise, the C-terminal FRF C-terminal motif was found to have homology with the N-terminal residues of cytochrome c oxidase from *Pseudomonas stutzeri* (Buschmann et al., 2010; Li et al., 2014) However, Ac78 and some of its orthologs do not contain a single cysteine, and every Ac78 ortholog does not contain the CXXC active site. Because of the conservation of baculoviral core genes, one can predict that homologs play similar functional roles in different systems. However, it has yet to be shown whether any key

differences arising from the evolution of *ac78* lead to slightly altered functional roles, and it is thus worthwhile to study the function of Ac78 in different baculoviral systems.

1.6 References

Albright BS, Kosinski A, Szczepaniak R, Cook EA, et al. (2015). The putative herpes simplex virus 1 chaperone protein UL32 modulates disulfide bond formation during infection. J Virol. 2015;89:443–453.

Argyrou, A., & Blanchard, J. S. (2004). Flavoprotein Disulfide Reductases: Advances in Chemistry and Function. *Progress in Nucleic Acid Research and Molecular Biology*,89-142. doi:10.1016/s0079-6603(04)78003-4

Barbouche R, Miquelis R, Jones IM, Fenouillet E. Protein-disulfide isomerase-mediated reduction of two disulfide bonds of HIV envelope glycoprotein 120 occurs post-CXCR4 binding and is required for fusion. Journal of Biological Chemistry. 2003;278:3131–3136.

Bardwell, J. C., Mcgovern, K., & Beckwith, J. (1991). Identification of a protein required for disulfide bond formation in vivo. *Cell,67*(3), 581-589. doi:10.1016/0092-8674(91)90532-4

Bauer, M. F., Hofmann, S., Neupert, W., & Brunner, M. (2000). Protein translocation into mitochondria: The role of TIM complexes. *Trends in Cell Biology,10*(1), 25-31. doi:10.1016/s0962-8924(99)01684-0

Bechtel, T. J., & Weerapana, E. (2017). From structure to redox: The diverse functional roles of disulfides and implications in disease. *Proteomics,17*(6), 1600391. doi:10.1002/pmic.201600391

Beek, N. V., & Davis, D. C. (2016). Baculovirus Insecticide Production in Insect Larvae. *Mehods Mol. Biol.*,393-405. doi:doi: 10.1007/978-1-4939-3043-2_20.

Bonsall, M. B. (2004). The impact of diseases and pathogens on insect population dynamics. *Physiological Entomology,29*(3), 223-236. doi:10.1111/j.0307-6962.2004.00389.x

Chen CY, Lin CY, Chen GY, Hu YC. (2011). Baculovirus as a gene delivery vector: recent understandings of molecular alterations in transduced cells and latest applications. Biotechnol Adv 29: 618–631.

Chen, L., Shen, Y., Yang, R., Wu, X., Hu, W., & Shen, G. (2015). Bombyx mori nucleopolyhedrovirus (BmNPV) Bm64 is required for BV production and per os infection. *Virology Journal,12*(1). doi:10.1186/s12985-015-0399-9

Condreay JP, Kost TA. (2007). Baculovirus expression vectors for insect and mammalian cells. Curr. Drug Targets 8:1126–1131

Cook KM & Hogg PJ. (2013). Post-translational control of protein function by disulfide bond cleavage. Antioxid Redox Signal. 18:1987–2015.

Clem, S. A., Wu, W., & Passarelli, A. L. (2014). The Trichoplusia ni single nucleopolyhedrovirus tn79 gene encodes a functional sulfhydryl oxidase enzyme that is able to support the replication of Autographa californica multiple nucleopolyhedrovirus lacking the sulfhydryl oxidase ac92 gene. *Virology,460-461*, 207-216. doi:10.1016/j.virol.2014.05.006

Darby, N. J., & Creighton, T. E. (1995). Functional properties of the individual thioredoxin-like domains of protein disulfide isomerase. *Biochemistry,34*(37), 11725-11735. doi:10.1021/bi00037a009

Deponte, M., & Hell, K. (2009). Disulphide Bond Formation in the Intermembrane Space of Mitochondria. *Journal of Biochemistry,146*(5), 599-608. doi:10.1093/jb/mvp133

Embley, T. M., & Martin, W. (2006). Eukaryotic evolution, changes and challenges. *Nature,440*(7084), 623-630. doi:10.1038/nature04546

Fass, D. (2008). The Erv family of sulfhydryl oxidases. *Biochimica Et Biophysica Acta (BBA) - Molecular Cell Research,1783*(4), 557-566. doi:10.1016/j.bbamcr.2007.11.009

Feige MJ & Hendershot LM. (2011). Disulfide bonds in ER protein folding and homeostasis. Curr Opin Cell Biol. 23:167–175.

Gabaldón T, Huynen MA. (2004). Prediction of protein function and pathways in the genome era. Cell. Mol. Life Sci. 61:930–944.

Gallot-Lavallée, L., & Blanc, G. (2017). A Glimpse of Nucleo-Cytoplasmic Large DNA Virus Biodiversity through the Eukaryotic Genomics Window. *Viruses,9*(1), 17. doi:10.3390/v9010017

Garavaglia MJ, Miele SAB, Iserte JA, Belaich MN, Ghiringhelli PD. (2012). The ac53, ac78, ac101, and ac103 genes are newly discovered core genes in the family Baculoviridae. J. Virol. 86:12069–12079. http://dx.doi.org/10.1128/JVI.01873-12.

Gilbert, H. F. (1990). Molecular and Cellular Aspects of Thiol-Disulfide Exchange. *Advances in Enzymology - and Related Areas of Molecular Biology Advances in Enzymology and Related Areas of Molecular Biology*,69-172. doi:10.1002/9780470123096.ch2

Glerum, D. M., Shtanko, A., & Tzagoloff, A. (1996). Characterization ofCOX17, a Yeast Gene Involved in Copper Metabolism and Assembly of Cytochrome Oxidase. *Journal of Biological Chemistry,271*(24), 14504-14509. doi:10.1074/jbc.271.24.14504

Gonnet, G., Cohen, M., & Benner, S. (1992). Exhaustive matching of the entire protein sequence database. *Science,256*(5062), 1443-1445. doi:10.1126/science.1604319

Hou D, Zhang L, Deng F, Fang W, Wang R, Liu X, Guo L, Rayner S, Chen X, Wang H. (2013). Comparative proteomics reveal fundamental structural and functional differences between the two progeny phenotypes of a baculovirus. J. Virol. 87:829–839. 10.1128/JVI.02329-12

Martignoni, M. E., and P. J. Iwai. (1981). A catalogue of viral diseases of insects, mites, and ticks, p. 897-911. *In* H. D. Burges (ed.), Microbial control of pests and plant diseases 1970-1980. Academic Press, Inc., London, United Kingdom.

International Committee on Taxonomy of Viruses (ICTV). (2017). Virus Taxonomy: 2013 Release, Edinburgh, Switzerland

Javed, M. A., Biswas, S., Willis, L. G., Harris, S., Pritchard, C., Oers, M. M., . . . Theilmann, D. A. (2016). Autographa californica Multiple Nucleopolyhedrovirus AC83 is a Per Os Infectivity Factor (PIF) Protein Required for Occlusion-Derived Virus (ODV) and Budded Virus Nucleocapsid Assembly as well as Assembly of the PIF Complex in ODV Envelopes. *Journal of Virology,91*(5). doi:10.1128/jvi.02115-16

Rohrmann, G. F. (2011). *Baculovirus molecular biology*. Bethesda, MD: National Library of Medicine, National Center for Biotechnology Information.

Podgwaite, J.D. (1981). *Natural disease within dense gypsy moth populations*, in *The Gypsy Moth: Research Towards Integrated Pest Management*, C.C. Doane and M.L. McManus, Editors. U.S. Dept. of Agriculture: Washington, D.C.

Myers, J. H., & Cory, J. S. (2015). Ecology and evolution of pathogens in natural populations of Lepidoptera. *Evolutionary Applications,9*(1), 231-247. doi:10.1111/eva.12328

Moscardi F. (1999). Assessment of the application of baculoviruses for control of lepidoptera. Annu. Rev. Entomol. 44:257–289.

Summers MD. (2006). Milestones leading to the genetic engineering of baculoviruses as expression vector systems and viral pesticides. Adv. Virus Res.68:3–73.

Kalha, C., Singh, P., Kang, S., Hunjan, M., Gupta, V., & Sharma, R. (2014). *Integrated Pest Management: Current Concepts and Ecological Management*. doi:https://doi.org/10.1016/B978-0-12-398529-3.00013-0

United States Environmental Protection Agency (EPA). (2016, December 11). Search by Chemical Name (Active Ingredients): NPV. Retrieved July 12, 2018, from https://iaspub.epa.gov/apex/pesticides/f?p=PPLS:17:::NO::

Kost TA, Condreay JP, Jarvis DL. (2005). Baculovirus as versatile vectors for protein expression in insect and mammalian cells. Nat. Biotechnol. 23:567–575.

Possee RD. (1997). Baculoviruses as expression vectors. Curr. Opin. Biotechnol.8:569–572

Hakim M., et al. (2011). Structure of a Baculovirus Sulfhydryl Oxidase, A Highly Divergent Member of the Erv Flavoenzyme Family. *J Virol.* 85(18): 9406-9413

Hakim, M., Ezerina, D., Alon, A., Vonshak, O., & Fass, D. (2012). Exploring ORFan Domains in Giant Viruses: Structure of Mimivirus Sulfhydryl Oxidase R596. *PLoS ONE,7*(11). doi:10.1371/journal.pone.0050649

Hakim, M., & Fass, D. (2010). Cytosolic Disulfide Bond Formation in Cells Infected with Large Nucleocytoplasmic DNA Viruses. *Antioxidants & Redox Signaling,13*(8), 1261-1271. doi:10.1089/ars.2010.3128

Hatahet F, Ruddock LW. (2009). Protein disulfide isomerase: a critical evaluation of its function in disulfide bond formation. Antioxid Redox Signal. 2009;11:2807–2850.

Herniou, E. A., Luque, T., Chen, X., Vlak, J. M., Winstanley, D., Cory, J. S., & Oreilly, D. R. (2001). Use of Whole Genome Sequence Data To Infer Baculovirus Phylogeny. *Journal of Virology,75*(17), 8117-8126. doi:10.1128/jvi.75.17.8117-8126.2001

Hoober, K. L., & Thorpe, C. (1999). Egg White Sulfhydryl Oxidase: Kinetic Mechanism of the Catalysis of Disulfide Bond Formation†. *Biochemistry,38*(10), 3211-3217. doi:10.1021/bi9820816

Huang, H., et al. (2014). The ha72 Core Gene of Baculovirus Is Essential for Budded Virus Production and Occlusion-Derived Virus Embedding, and Amino Acid K22 Plays an Important Role in Its Function. *Journal of Virology*, vol. 88, no. 1, pp. 705–709

Jones, D. T., Taylor, W. R., & Thornton, J. M. (1992). The rapid generation of mutation data matrices from protein sequences. *Bioinformatics,8*(3), 275-282. doi:10.1093/bioinformatics/8.3.275

Landeta, C., Boyd, D., & Beckwith, J. (2018). Disulfide bond formation in prokaryotes. *Nature Microbiology,3*(3), 270-280. doi:10.1038/s41564-017-0106-2

Li, Sai-Nan, et al. (2014). Disruption of the baculovirus core gene ac78 results in decreased production of multiple nucleocapsid-Enveloped occlusion-derived virions and the failure of primary infection in vivo. *Virus Research*, vol. 191, pp. 70–82.

Long C.M., Rohrmann G.F., Merrill G.F. (2009). The conserved baculovirus protein p33 (Ac92) is a flavin adenine dinucleotide-linked sulfhydryl oxidase. *Virology.* 388(2): 231–5.

Maghodia, A. B., Jarvis, D. L., & Geisler, C. (2014). Complete Genome Sequence of the Autographa californica Multiple Nucleopolyhedrovirus Strain E2. *Genome Announcements,2*(6). doi:10.1128/genomea.01202-14

Matthias LJ, Yam PT, Jiang XM, Vandegraaff N, et al. (2002). Disulfide exchange in domain 2 of CD4 is required for entry of HIV-1. Nat Immunol. 3:727–732.

Miller, L. K., & Lu, A. (1997). The Molecular Basis of Baculovirus Host Range. *The Baculoviruses,*217-235. doi:10.1007/978-1-4899-1834-5_9

Nie, Yingchao, et al. (2011). Autographa californica multiple nucleopolyhedrovirus core gene ac92 (p33) is required for efficient budded virus production. *Virology*, vol. 409, no. 1, pp. 38–45.

Oliveira, J., Brito, A. D., Braconi, C., Freire, C. D., Iamarino, A., & Zanotto, P. D. (2013). Modularity and evolutionary constraints in a baculovirus gene regulatory network. *BMC Systems Biology,7*(1), 87. doi:10.1186/1752-0509-7-87

Rubinstein, R., & Fiser, A. (2008). Predicting disulfide bond connectivity in proteins by correlated mutations analysis. *Bioinformatics,24*(4), 498-504. doi:10.1093/bioinformatics/btm637

Saaranen MJ, Ruddock LW. (2013). Disulfide bond formation in the cytoplasm. Antioxid Redox Signal. 19:46–53.

Senkevich, T. G., Koonin, E. V., White, C. L., & Moss, B. (2000). A viral member of the ERV1/ALR protein family participates in a cytoplasmic pathway of disulfide bond formation. *Proc Natl Acad Sci,97*(22), 12068-12073. doi:10.3410/f.1002057.28105

Senkevich, T. G., White, C. L., Koonin, E. V., & Moss, B. (2002). Complete pathway for protein disulfide bond formation encoded by poxviruses. *Proceedings of the National Academy of Sciences,99*(10), 6667-6672. doi:10.1073/pnas.062163799

Sevier CS, Kaiser CA. (2002). Formation and transfer of disulphide bonds in living cells. Nat Rev Mol Cell Biol. 3:836–847.

Stojanovski, D., Müller, J. M., Milenkovic, D., Guiard, B., Pfanner, N., & Chacinska, A. (2008). The MIA system for protein import into the mitochondrial intermembrane space. *Biochimica Et Biophysica Acta (BBA) - Molecular Cell Research,1783*(4), 610-617. doi:10.1016/j.bbamcr.2007.10.004

Taha, A., Giannotti, J., Cry, X. L., Ravàlec, M., & Abol-ELA, S. (1995). Host Range of the Autographa californica multicapsid nuclear polihedrosis virus (AcMNPV) in relation to granulosis viruses susceptible Lepidopteran species in Egypt. *Egyptian Journal of Biological Pest Control,5*(2), 127-130.

Tao, X. Y., et al. (2013). The Autographa californica Multiple Nucleopolyhedrovirus ORF78 Is Essential for Budded Virus Production and General Occlusion Body Formation. *Journal of Virology*, vol. 87, no. 15, pp. 8441–8450.

Vail P., et al. (1971). Recipocal infectivity of nuclear polyhedrosis viruses of the cabbage looper and alfalfa looper. *J Invertebr Pathol*. 17:383–388.

Wong, J. W., Ho, S. Y., & Hogg, P. J. (2010). Disulfide Bond Acquisition through Eukaryotic Protein Evolution. *Molecular Biology and Evolution,28*(1), 327-334. doi:10.1093/molbev/msq194

Wrobel, L., Sokol, A. M., Chojnacka, M., & Chacinska, A. (2016). The presence of disulfide bonds reveals an evolutionarily conserved mechanism involved in mitochondrial protein translocase assembly. *Scientific Reports,6*(1). doi:10.1038/srep27484

Wu, W., and A. L. Passarelli. (2010). Autographa californica Multiple Nucleopolyhedrovirus Ac92 (ORF92, P33) Is Required for Budded Virus Production and Multiply Enveloped Occlusion-Derived Virus Formation. *Journal of Virology*, vol. 84, no. 23, pp. 12351–12361.

Chapter 2 - Defining the relationship between a baculoviral sulfhydryl oxidase and a potential accessory protein

2.1 Introduction

Baculoviridae is a large, diverse, and an ecologically-important family of entomopathogens that naturally infect the larvae of over 600 species of lepidopteran, dipteran, and hymenopteran insects (Martignoni, 1981). Baculoviral genomes are circular, double-stranded DNA (dsDNA) and range from 80 to 180 kilobase pairs (kbp) in length (Rohrmann, 2008). The genome is packaged in rod-shaped nucleocapsids surrounded by an outer lipid envelope (Akermann & Smirnoff, 1983; Federici, 1986). Two types of baculoviral virions are produced at different stages of the replication cycle: BV, which spreads the infection from cell-to-cell within the host, and ODV, which is highly stable in the outside environment and used to spread infection from host-to-host. While in the environment, ODV are found in occlusion bodies, which are crystalline matrixes composed of a protein called polyhedrin in nucleopolyhedroviruses (NPVs). Aggregated within the highly stable occlusion bodies, ODV can remain infectious in the environment for long periods of time. The baculovirus replication cycle begins when the host ingests occlusion bodies, which dissolve in the midgut, releasing ODV that infects midgut epithelial cells. Subsequently, BV buds out of the basal side of the infected cell and establishes systemic infection throughout the host. Late in infection, ODV is produced and aggregated into occlusion bodies. Upon cell death, occlusion bodies are released back into the environment until ingested by a new host individual.

AcMNPV is the prototype baculovirus originally described as a pathogen of the alfalfa looper moth (*Autographa californica*) in the 1970s (Vail et al., 1971). AcMNPV contains 38 core genes (Garavaglia et al., 2012; Javed et al., 2017) that are conserved among all of the 88 baculoviruses sequenced to date. This conservation indicates an essential role of each of the core genes in the viral replication cycle. One such core gene is *ac78* (Figure 2.1). Ac78 is associated with the envelope in ODV. When *ac78* was deleted from AcMNPV, viral DNA replication appeared to be unaffected; however, nucleocapsids were confined to the nucleus, and BV and ODV-embedded occlusion bodies were not produced or produced in very low levels (Tao et al., 2013; Li et al., 2014). While it is clear that Ac78 plays an important function in the AcMNPV replication cycle, the biochemical mechanism by which Ac78 is involved in the production of virions has not previously been shown. One focus of this thesis project was to fill this knowledge gap by elucidating the molecular mechanism by which Ac78 is essential in the production of virions.

Another essential conserved gene in baculoviruses is *ac92*, which is a flavin adenine dinucleotide (FAD)-linked sulfhydryl oxidase gene that is conserved in all known baculoviruses to date but not commonly found in other virus families (Long et al., 2009; Wu & Passarelli, 2010). Ac92 is present in the envelope of BVs and ODVs and its function is essential for the viral replication cycle. Published results from the laboratory of Dr. Lorena Passarelli show that both deletion of *ac92* from AcMNPV or mutation of the cysteine residues to alanines in the active site of Ac92 is essential for viral replication (Wu & Passarelli, 2010) and results in phenotypic changes that are strikingly similar to that of AcMNPVs lacking *ac78* (Tao et al., 2013; Li et al., 2014). When *ac92* was deleted from AcMNPV, viral DNA replication was unaffected, infectious BV was not produced, and the ODV consisted of singly-enveloped virions instead of the multiply-enveloped nucleocapsids normally found in AcMNPV (Wu & Passarelli, 2010). Recently, the Ac78 and

Ac92 homologs in Helicoverpa armigera nucleopolyhedrovirus (HearNPV) were reported to interact and co-localize to the site of BV and ODV formation (Huang et al., 2014).

To investigate the relationship between Ac78 and Ac92, we determined their localization in the presence and absence of AcMNPV infection, performed co-immunoprecipitation to assess interaction relationships, and provided an updated report of Ac78 and Ac92 homology with other proteins. We concluded that in the absence of viral infection, Ac78 and Ac92 localized perinuclearly in the cytoplasm and that localization of Ac92 was not affected by the exogenous presence (pAc78^{HA}-transfected) or absence of *ac78*. During AcMNPV infection, Ac78 and Ac92 co-localized within the nucleus and surrounding virus replication and assembly sites (ring zone). Co-immunoprecipitation experiments showed that at least two differentially-tagged Ac78 proteins were part of a complex in the presence of other AcMNPV proteins. Ac78 did not associate with Ac92 during AcMNPV infection. Ac78 did not immunoprecipitate with Ac92 at late timepoints during AcMNPV infection. Our characterization of the relationship between Ac78 and the AcMNPV sulfhydryl oxidase is a preliminary step in a broader effort to elucidate important biochemical pathways underlying the poorly described structural changes in capsid proteins and other proteins involved in virion stability, folding, and infectivity.

2.2 Materials and methods

Viruses and cell lines

The Sf9 insect cell line, clonal isolate 9 from IPLB-Sf21-AE cells, is derived from the fall armyworm *Spodoptera frugiperda*. The Sf9 cell line was purchased from ATCC and cultured at 27°C in TC-100 medium from Invitrogen supplemented with 10% fetal bovine serum (Atlanta Biologicals), penicillin G (60 μg/ml), streptomycin sulfate (200 μg/ml), and amphotericin B (0.5 μg/ml).

The repair bacmid containing Ac92 with an eGFP fusion protein expressed under the IE1 promoter, vAc92GFP, was constructed as previously described (Wu et al., 2013).

The bacmid containing AcMNPV expressing the polyhedron gene, AcMNPV-PH, was constructed as previously described (Wu et al., 2013).

The repair bacmid in which AcMNPV with endogenous Ac92 knocked out and replaced with C-terminally-Flag-tagged Ac92, vAc92FLAG, was constructed as previously described (Wu et al., 2013).

Construction of plasmids

Plasmid pAc78HA, an expression construct for Ac78 containing a C-terminal hemagglutinin (HA) tag expressed under the Drosophila heat shock promoter (hsp70), which drives protein expression in cells after exposure to heat shock conditions (42°C), was constructed. AcMNPV-PH bacmid DNA was used as a template for PCR with a forward primer containing Bsu36I restriction site (5'-CCGGCCTAAGGATGAATTTGGACGTGCCCTAC-3') and a reverse primer containing the HA sequence and the Bsu36I restriction site (5'-GGCCCCTAAGGTTATGCATAATCCGGAACATCATACGGATAATCAAATTTATTAAA-

3'). The PCR product was purified, digested with Bsu36I (New England BioLabs, Ipswich, MA), and purified again. A plasmid containing the GFP open reading frame expressed under the hsp70 promoter was digested using Bsu36I to remove the GFP fragment, concurrently digested with Bsu36I and dephosphorylated with Shrimp Alkaline Phosphatase (New England Biolabs, Ipswich, MA), and gel purified (Qiagen,Valencia, CA). The digested purified PCR product was ligated with the Bsu36I-linearized phsp70 vector. The construct was then ligated with the digested PCR insert to yield the final construct pAc78^{HA}. Ligation products were transformed into XL1 Blue competent cells (Stratagene, La Jolla, CA), and bacteria were plated on LB-ampicillin-agar plates and incubated at 37°C for 14 to 20 hours. Single colonies were selected and grown in 2 mL LB-ampicillin, and plasmids were extracted using a plasmid minikit (Qiagen,Valencia, CA) and analyzed by restriction endonuclease digestion and electrophoresis. Three clones containing the expected insert size were subjected to Sanger sequencing using a forward primer located in the hsp70 promoter (5'-CTGCAACAACTGAAATCAACCAAGAAGTC-3'), and one clone containing a single insert was selected for further experiments.

Plasmid pAc78FLAG, an expression construct for Ac78 containing a C-terminal Flag tag expressed under the Drosophilia hsp70 promoter, was constructed. The plasmid pAc78HA was used as a template for PCR with a forward primer containing a Bsu36I restriction site (5'-CCGGCCTAAGGATGAATTTGGACGTGCCCTAC-3') and a reverse primer containing the Flag sequence and a Bsu36I restriction site (5'-GGCCCCTAAGGTTACTTGTCGTCATCGTCTTTGTAGTCATCAAATTTATTAAA-3'). The PCR product was purified, digested with Bsu36I (New England BioLabs, Ipswich, MA), and purified again. The Bsu36I-digested, purified PCR product was ligated with the Bsu36I-

linearized phsp70 vector, and an individual clone containing the proper insert sequence was obtained using the same methods described above for the cloning of pAc78HA.

The plasmid containing Ac92 with an enhanced GFP fusion protein expressed under the IE1 promoter, pAc92GFP, was constructed as previously described (Wu et al., 2013).

Plasmid or bacmid DNA transfections

To transfect plasmid or bacmid DNA, DNAs were mixed with a non-commercial liposome reagent and added to Sf9 cells as previously described (Crouch and Passarelli, 2002). Cells were incubated with the DNA/liposome mixture in unsupplemented Grace's Insect Medium (Thermo Fischer Scientific, Waltham, MA) at 27°C for 5 hours and then washed twice with unsupplemented Grace's media, followed by addition of TC-100 media containing 10% fetal bovine serum (designated as the zero-time point) and incubation at 27°C.

Immunofluorescence

Immunofluorescence allowed us to visualize and quantify the localization of Ac78 and Ac92 in Sf9 cells in the presence and absence of AcMNPV infection. The plasmids pAc78HA and pAc92GFP and the viruses vAc92GFP and AcMNPV-PH were utilized for this purpose. An amount of 2.5 μL of the indicated plasmid, bacmid, or combinations thereof were co-transfected using the methods described above into 1 x 10^6 Sf9 cells seeded onto cover slips in 35 mm dishes 24 hours before transfection. At the indicated time points, the supernatant was removed and the cells were washed twice with PBS, pH 6.2 (Potter and Miller, 1980), fixed in Formalde-Fresh 4% formaldehyde solution (Fisher Scientific, Waltham, MA) for 10 minutes at room temperature (RT), and washed for 5 minutes in PBS three times. Fixed cells were permeabilized in 0.3%

Triton X-100 (Sigma-Aldrich, St. Louis, MO) in PBS for 10 min at RT, washed for 5 minutes in PBS three times, blocked in 5% BSA in PBS for 1 hour at RT, and incubated overnight at 4°C in anti-HA.11 antibody (BioLegend, San Diego, CA) at a concentration of 1:1000 in PBS containing 1% BSA in order to bind HA-tagged Ac78. Cells were washed for 5 minutes in PBS three times, followed by incubation with Alexa Fluor 633-conjugated anti-mouse IgG antibody (Thermo Fisher, Waltham, MA) in the dark for 1 hour at RT. Cells were washed for 5 minutes in PBS three times and then incubated with 1:70,000 dilution of SYTOX Orange (Thermo Fisher, Waltham, MA) in PBS in the dark for 10 minutes at RT. The cells were washed for 5 minutes in PBS three times, and coverslips were mounted on a glass slide and stored at 4°C in the dark until examined with a Carl Zeiss LSM 5 Pascal Laser Scanning Confocal Microscope.

Co-immunoprecipitation assays

A co-immunoprecipitation technique (as described in Lehiy et al., 2013) allowed us to test whether Ac78 physically associated with itself in the presence or absence of AcMNPV and whether Ac78 associated with Ac92 in the presence of AcMNPV. Two plasmids containing the following genes expressed under the hsp70 promoter were constructed as described above: pAc78HA and pAc78FLAG. Additionally, an AcMNPV containing Flag-tagged Ac92 (vAc92FLAG) was utilized. An amount of 2.5 μL of the indicated plasmids was co-transfected into Sf9 cells. At 20 hours post transfection (h.p.t.), 50 ug/mL of MG-132 was added to uninfected samples to block degradation of the desired proteins through the 26S proteasome, and 30 minutes after the addition of MG-132, cells were heat shocked for 30 minutes at 42°C in order to drive expression under the heat shock promoter. Alternatively, transfected cells were infected at a multiplicity of infection (MOI) of 5 plaque forming units (PFU)/mL with

vAc92FLAG or AcMNPV-PH at 18 h.p.t. At 24 h.p.t. or 48 hours post-infection (h.p.i.), transfected and/or infected cells were pelleted at 2000 xg for 3 min and lysed with NP-40 IP/lysis buffer (50 mM Tris–HCl, pH 8.0; 150 mM NaCl; 1 mM EDTA; 1% NP-40) and two cycles of freeze-thawing. The lysate was clarified by centrifugation at 10,000 xg for 5 minutes and precleared by adding 50 µ l of a 50% slurry of protein G beads (Sigma), followed by incubation at 4°C for 1 hour with rolling. The supernatant was then transferred to a new microcentrifuge tube and mixed with anti-Flag antibody. After incubation at 4°C for 3 hours with rolling, 50 µl of a 50% slurry of protein G beads was added to the mixture and incubated for another 1 hour at 4°C with rolling. The beads were collected by centrifugation and washed five times with IP/lysis buffer for 15 min each. Following addition of 25 µl of 2x Protein Loading Buffer (PLB, 0.25 M Tris–Cl, pH 6.8, 4% SDS, 20% glycerol, 2% 2-mercaptoethanol and 0.02% bromophenol blue), the samples were heated at 100°C for 5 min. Samples were immediately analyzed by immunoblotting or stored at −80°C until use.

Immunoblotting

Cells were collected and washed with PBS, pH 6.2 (Potter and Miller, 1980), resuspended in PBS with an equal volume of 2X PLB, and incubated at 100 C for 5 min. Protein samples were resolved by SDS-14% PAGE, transferred onto a PVDF membrane (Millipore-Sigma), and probed with one of the following primary antibodies: anti-HA.11 monoclonal mouse IgG antibody (BioLegend, San Diego, CA) or anti-FLAG mouse monoclonal antibody (Sigma Aldrich, St. Louis, MO), followed by incubation with anti-mouse horse radish peroxidase-conjugated secondary antibodies (Cell Signaling, Danvers, MA). Blots were developed using

SuperSignal West Pico Chemiluminescent substrate (Thermo Fisher, Waltham, MA) and exposed on an Azure Biosystems C600 imaging machine.

2.3 Results

2.3.1 Comprehensive sequence comparison of 80 baculoviral FAD-linked sulfhydryl oxidases

In order to gain insight into the function of Ac78, we entered the AcMNPV Ac92 protein sequence into NCBI BLAST to obtain the sequences of 79 of its baculovirus homologs and performed multiple sequence alignment using Clustal Omega software (Figure 2.1). The results showed highly conserved amino acid residues clustered throughout the full-length amino acid sequence. The active sites in the Erv-family sulfhydryl oxidase motif were highly conserved among all groups of baculoviruses; our results showed that 100% of the Ac92 orthologs analyzed contained the CXXC motif at the amino terminus of the proteins. A sequence that is predicted to contribute to the binding of the FAD and consists of a tryptophan, three histidine, and two asparagine amino acid residues ($WX_3HX_nHX_mHNX_2N$) was 100% conserved in all analyzed baculoviruses, with the exception of a Y being present at the site of the last H in CuniNPV. BLAST searches using the full-length Ac92 protein sequence did not result in cellular or viral protein hits from outside of baculoviruses.

2.3.2 Sequence comparison of Ac78 and its orthologs

In order to gain insight into the function of Ac78, we entered the AcMNPV Ac92 protein sequence into NCBI BLAST to obtain the sequences of 79 of its homologs and performed sequence alignment using Clustal Omega software (Figure 2.2). Our results showed the

conservation of the two recognized motifs of Ac78, an IPLKL motif and a putative fumarate reductase flavoprotein (FRF) C-terminal motif (Huang et al., 2014), among its homologs in previously- and newly-sequenced baculovirus species and strains. The IPLKL motif, which is known to function as a peroxisome signaling site in plants (Raychaudhuri & Tipton, 2002), was found to be highly conserved among all four baculoviral groups. It was recently reported by Huang et al., 2014 that the middle lysine in the IPLKL motif was essential for Ac78 function in the production of virions. Interestingly, our multiple sequence alignment showed three baculoviruses for which an arginine was present at the middle lysine site. The FRF C-terminal motif, which has been implemented in redox signaling in some nonviral systems, was found to be highly conserved among the alphabaculoviruses and two recently-discovered viruses that have yet to be assigned to a group. Our multiple sequence alignment showed that the FRF C-terminal motif of the betabculoviruses is highly conserved among the betabaculoviruses but with different amino acid residues from the alphabaculoviruses. The motif diverges even further in gammabaculoviruses and the fully-sequenced deltabaculovirus (CuniNPV). Additionally, Ac78 and its homologs contain a transmembrane motif (amino acids 61-83 of Ac78). However, the specific identity of the amino acids is not conserved at the transmembrane motif site other than containing an increased number of the nine hydrophic amino acids. The authors of Huang et al., 2014 proposed a hypothesis that Ac78 may act together with the sulfhydryl oxidase during redox processes. Our alignment shows that Ac78 does not contain two cysteine residues in close proximity to one another (CXXC). Roughly half of the alphabaculoviruses contain a single cysteine in the FRF C-terminal motif and no additional cysteines throughout the protein sequence. While the presence of this single cysteine indicates that the Ac78 orthologs could potentially participate in intermolecular disulfide bonding, the lack of a CXXC active site

indicates that Ac78 nor its orthologs likely serve as oxidoreductases with Ac92. It is possible that Ac78 may instead be a downstream substrate of an Ac92-catalyzed oxidoreduction pathway.

2.3.3 Ac78 and Ac92 may contain predicted cytoplasmic and nuclear localization signals

It has previously been reported that Ac92 localizes perinuclearly in the cytoplasm in the absence of other AcMNPV proteins but localizes within the nucleus and around the viral DNA replication area (ring zone) during AcMNPV infection (Nie et al., 2011; Wu et al., 2013). These findings suggest that another AcMNPV protein is necessary for the localization of Ac92 to the nucleus. However, the protein(s) responsible for the nuclear localization of Ac92 have not been identified. We hypothesized that one function of Ac78 may be to localize Ac92 to the nucleus. To gather more insight, we performed an *in silico* search for nuclear localization sequences in Ac78 and Ac92 using cNLS Mapper software (Kosugi et al., 2009). The cNLS mapper predicts nuclear localization sequences (NLSs) specific to the importin α/β pathway by calculating NLS scores with four NLS profiles, each of which represents a contribution of every amino acid residue at every position within an NLS class to the entire NLS activity. Extensive amino acid replacement analysis in budding yeast was used to give positive or negative contribution scores to each amino acid residue, which additively or independently contributes to the overall nuclear localization activity of the sequence. This led to four NLS classifications: exclusive nuclear localization, partial nuclear localization, nuclear and cytoplasmic localization, and exclusive cytoplasmic localization. Results from this search showed that Ac92 and Ac78 contained predicted NLS sequences with scores of 3.6 and 3.7, respectively. A GUS-VFP reporter protein fused to an NLS with a score of 3-5 localized to both the nucleus and the cytoplasm. Thus, both Ac78 and Ac92

contained sequences predicted by the cNLS mapper to have both cytoplasmic and nuclear localization. The cNLS Mapper predicted moderate bipartite nuclear localization sequences with a similar score in Ac78 and Ac92 homologs, including those found in HearNPV.

It should be emphasized that the cNLS mapper prediction is based on the importin α/β nuclear import pathway in budding yeast. While the importin α/β nuclear import pathway is highly conserved among eukaryotes, the prediction of the cNLS mapper based on yeast may not be as effective in our insect species.

2.3.4 Ac78 did not affect the cellular localization of Ac92 and partially co-localized with Ac92 in Sf9 cells

To determine the localization of Ac78 and whether Ac78 affects the localization of Ac92 in the absence of other viral proteins in insect cells, we performed immunofluorescence experiments in Sf9 cells transfected with plasmids pAc78^{HA}, visualized with an anti-HA.11 mouse primary antibody and Alexa Fluor 633-conjugated anti-mouse secondary antibody, and pAc92^{GFP}, visualized through its eGFP fusion tag. SYTOX Orange nuclear stain was used to visualize DNA in the nucleus, where viral DNA replicates. In the absence of other viral proteins, Ac92 produced from pAc92^{GFP} localized mainly in a punctate staining pattern perinuclear with some additional diffuse staining throughout the rest of the cytoplasm of pAc92GFP-transfected cells. Ac78 produced from pAc78^{HA} localized as a diffused uniform ring perinuclear in the cytoplasm with some additional diffuse staining throughout the rest of the cytoplasm of pAc78HA-transfected cells. The staining patterns of neither Ac78 nor Ac92 changed in pAc92GFP/pAc78HA co-transfected cells, and some areas of co-localization were observed (Figure 2.4).

We additionally determined localization of Ac78 in the presence of AcMNPV infection and corroborated results of the localization of Ac92 in the presence of AcMNPV infection utilizing the plasmid pAc78-HA and viral DNA from AcMNPV-PH or vAc92GFP. In cells co-transfected with pAc78HA and vAc92-GFP, Ac92 and Ac78 co-localized in the nucleus around the viral DNA replication center (ring zone). Similar localization pattern was observed when pAc78HA was co-transfected with untagged AcMNPV-PH and when vAc92^{GFP} was transfected individually into insect cells.

2.3.5 Co-immunoprecipitation of Ac78 and Ac92

Co-immunoprecipitations were used to test whether Ac78 and Ac92 associate during AcMNPV infection. Our results showed that HA-tagged Ac78 expressed from the plasmid pAc78HA and FLAG-tagged Ac92 expressed from the virus vAc92FLAG did not precipitate when infected cells were collected at 48 h.p.i., lysed, immunoprecipitated on IgG beads using an anti-FLAG antibody, and analyzed with Western Blot analysis. These results indicated that Ac78 did not associate with Ac92 during AcMNPV infection under the conditions tested.

We additionally sought to determine whether more than one Ac78 molecule associates in a complex in the presence or absence of other AcMNPV proteins. Our results show that in the presence of AcMNPV proteins, HA-tagged Ac78 expressed from the plasmid pAc78HA co-precipitated with FLAG-tagged Ac78 expressed from the plasmid pAc78FLAG. In the absence of other AcMNPV proteins, pAc78HA and pAc78FLAG did not co-precipitate. These results indicate that at least two differentially-tagged Ac78 proteins were part of a complex in the presence of other AcMNPV proteins.

2.4 Conclusions

From our updated sequence alignments of Ac92 and its homologs, we concluded that Ac92 is highly conserved among baculoviral genomes and remains a core gene when including a number of newly sequenced baculovirus genomes. To date, 100% of the Ac92 orthologs conserved the CXXC motif at the amino terminus of the proteins. A motif that is predicted to contribute to the binding of the FAD and consists of a tryptophan, three histidine, and two asparagine amino acid residues ($WX_3HX_nHX_mHNX_2N$) is also 100% conserved in all analyzed baculovirus Ac92 sequences, with the exception of a Y being present at the site of the last H in the deltabaculovirus (CuniNPV).

From our updated multiple sequence alignment of Ac78 and its homologs, we concluded that the IPLKL and FRF C-terminal motifs are highly conserved among 80 sequenced baculovirus genomic sequences analyzed. We conclude that three baculoviruses in which the key lysine of the IPLKL motif was mutated to an arginine. Our alignments showed that three Ac78 sequences did not have the middle lysine in the IPLKL motif. The FRF C-terminal motif is additionally conserved among the betabaculoviruses, but the betabaculoviruses contain a number of differences from the alphabaculoviruses. Our BLAST results show that the full-length sequence of Ac78 and its orthologs remain unique to baculoviruses.

From our immunofluorescence experiments, we concluded that Ac78 and Ac92 localized perinuclearly in the cytoplasm of transfected insect cells in the absence of other AcMNPV proteins. From the results that $Ac92^{GFP}$ localization was the same in the presence ($pAc78^{HA}$-transfected) or absence of *ac78*, we additionally concluded that the localization of Ac92 in the absence of other viral proteins in not affected by Ac78. We conclude that Ac92 and Ac78 co-

localized within the nucleus and around the viral DNA replication area (ring zone) during AcMNPV infection. Our results corroborate previous reports of the localization of Ac78 and its homologs (Li et al., 2014; Huang et al., 2014) and Ac92 and its homologs (Prikhod'ko et al., 1999; Wu et al., 2013; Huang et al., 2014) during viral infection. Since both $Ac78^{HA}$ and $Ac92^{GFP}$ were mainly cytoplasmic in $pAc78^{HA}$- or $pAc92^{GFP}$-transfected cells and mainly nuclear in infected cells, we conclude that additional factors resulting from AcMNPV infection are necessary for the trafficking of Ac78 and Ac92 into the nucleus.

From our co-immunoprecipitation experiments, we conclude that at least two differentially-tagged Ac78 proteins were part of a complex in the presence of other AcMNPV proteins. We propose possible models for a protein complex that contains at least two Ac78 molecules (Table 2.2). Contrary to results reported in the HearNPV system (Huang et al., 2014) we concluded from out immunoprecipitation results that Ac78 did not associate with Ac92 during AcMNPV infection. However, additional methods such as yeast-two-hybrid assays will be necessary to confirm this result.

Overall, we conclude that our characterization of the relationship between Ac78 and the AcMNPV sulfhydryl oxidase is a preliminary step in a broader effort to elucidate important biochemical pathways underlying the poorly described structural changes in capsid proteins and other proteins involved in virion stability, folding, and infectivity.

2.5 Discussion

Overall, the Ac92 amino acid sequence was highly conserved among baculovirus sequences of all groups. The noncatalytic regions are highly divergent from other viral and cellular sulfhydryl

oxidases. However, the active site of the Ac92 Erv family sulfhydryl oxidase region contains amino acid sequences shared by other sulfhydryl oxidases in cellular and viral systems. In particular, our results showed that 100% of the baculoviral sulfhydryl oxidases analyzed contained the CXXC motif at the amino terminus of the amino acid sequence. This CXXC motif is known form a helix and corresponds to the active site disulfide implemented in redox reactions. A motif that is predicted to contribute to the binding of the active site for the FAD and consists of a tryptophan, three histidine, and two asparagine amino acid residues ($WX_3HX_nHX_mHNX_2N$) was conserved in over 80% of analyzed baculoviruses. Additional highly conserved amino acid residue sites were clustered throughout the full-length amino acid sequence. While full-length Ac92 is unique to baculoviruses, its Erv-family active site is found in other viral and cellular proteins. One hypothesis is that Ac78 may be required for the oxidation of substrates.

The high conservation of the IPLKL motif of Ac78 homologs indicates an essential function. It is known that the IPLKL motif is involved in peroxisome signaling in plants (Raychaudhuri & Tipton, 2002). One hypothesis is that the IPLKL motif is essential for the signaling of Ac78 to localize to the necessary sites of action during infection. The FRF motif has been shown to play a role in redox processes in non-viral systems (Fritz et al., 2002; Mattevi et al., 1999). One hypothesis proposed by the authors of Huang et al., 2014 is that Ac78 may have enzymatic functions in redox processes along with the sulfhydryl oxidase. The results of our multiple sequence alignment showed that Ac78 and its homologs do not contain two cysteine residues in close proximity of one another (i.e., a CXXC motif). Further, AcMNPV and ~1/3 of its orthologs do not contain any cysteine residue.

Our results that Ac78 and Ac92 localized within the nucleus and surrounding virus replication and assembly sites (ring zone) during AcMNPV infection suggested that both proteins may play structural roles in the production of new virions. This finding was in-line with a previous report that Ac92 localizes in a punctate staining pattern in the cytoplasm around the outside of the nucleus (Wu et al., 2014) and provided new information regarding the localization of Ac78 that further supports a direct involvement of Ac78 in BV and ODV formation and provides one additional step in explaining why AcMNPVs that lack Ac78 have nonexistent or severely impaired BV and ODV formation. The co-localization of Ac78 and Ac92 in the presence of AcMNPV meant that the two proteins may or may not require other products or factors resulting from viral infection to co-localize. To gain insight on nuclear localization of Ac78 and Ac92, we searched for nuclear localization sequences (NLS) within the Ac78 and Ac92 amino acid sequences. Results from this search suggested that Ac92 and Ac78 contain sequences that may predict both cytoplasmic and nuclear localization. Because the nuclear cNLS mapper is based on the importin α/β pathway in budding yeast, this prediction may or may not hold in insectile systems. In the absence of AcMNPV infection, our results showed that p-Ac92^{GFP}-transfected cells exhibited punctate staining pattern perinuclear with some additional diffuse staining throughout the rest of the cytoplasm. Likewise, pAc78^{HA}-transfected cells exhibited punctate staining pattern perinuclear with some additional diffuse staining throughout the rest of the cytoplasm. The staining patterns of neither Ac78 nor Ac92 changed in pAc92GFP/pAc78HA co-transfected cells, and some areas of co-localization were observed. This partial co-localization is likely due to the fact that the two proteins localize to those areas and not due to their presence influencing one another. Additionally, these results indicate that additional factors resulting from viral infection are required to localize Ac78 and Ac92 to the nucleus. This could be due to

another viral protein shuttling them to the nucleus, changes to the cellular environment of the host resulting from baculoviral modulation of host proteins and gene expression, or a combination of both.

We hypothesized that Ac78 and Ac92 may interact during AcMNPV infection due to 1. the prior knowledge that infection of insect cells with AcMNPV lacking Ac92 results in similar phenotypes to infection with AcMNPV lacking Ac78, 2. our recently-obtained results that Ac78 and Ac92 co-localized at the site of viral replication and virion formation during AcMNPV infection, and 3. the report that Ac78 and Ac92 homologs of the baculovirus HearNPV interacted in yeast-two-hybrid assays. Because of the conservation of *ac78* and *ac92* between AcMNPV and HearNPV, we reasoned that Ac78 and Ac92 may have the same function(s) in the two different systems. Thus, the preliminary finding reported here that Ac78 did not associate with Ac92 during AcMNPV infection was not expected. Several possibilities may explain this result. The first possibility is that an inherent limitation of transfection experiments did not allow for the detection of the Ac78-Ac92 complex. It is possible that Ac78 and Ac92 do not interact in the reducing environment of the cytoplasm and instead only interact within the nucleus during a specific time during viral infection. The nucleus is not lysed with the detergent NP-40 commonly used for co-immunoprecipitation applications. Thus, a complex in which Ac78 and Ac92 are a part of may not be detectable using NP-40 buffer. It is additionally possible that Ac78 and Ac92 form a weak or transient interaction during viral infection and that this interaction is disrupted or does not occur at the time points at which the lysates were collected for the experiments. Other techniques, such as yeast-two-hybrid assays, would be necessary for determining whether Ac78 and Ac92 interact in the absence of other intermediate viral proteins. A second, less likely possibility is that Ac78 and Ac92 do not interact in the AcMNPV system. AcMNPV is a type I

alphabaculovirus, whereas HearNPV is a type II baculovirus. Type I and type II alphabaculoviruses differ in having additional and absent genes from one another. Thus, it is highly unlikely but still possible that Ac78, despite being a core gene, may have slightly different function in the AcMNPV system.

Our result that two differentially tagged Ac78 proteins co-precipitated in the presence of AcMNPV infection but not when transfected in isolation of AcMNPV infection indicates that at least two different Ac78 molecules were part of a complex in the presence of other AcMNPV proteins. Several scenarios could explain this result (Table 2.2). One scenario is that another viral protein is responsible for bridging two or more Ac78 molecules together. Alternatively, a cellular protein could be modulated by viral infection, such as by phosphorylation or methylation, and undergo conformational changes to permit two or more Ac78 molecules to interact. A third possibility is that a complex of viral and cellular proteins form of which two or more molecules of Ac78 are part of. Overall, this work is a first step in determining a physical model of the complex that these two important proteins may form

2.6 Future direction

The co-immunoprecipitation results that Ac78 and Ac92 did not associate during AcMNPV infection is contrary to previously reported in another baculoviral system (Huang et al., 2014). Testing the interaction of Ac78 and Ac92 using yeast-two-hybrid assays and FRET analysis is a necessary further step in order to corroborate the results shown in our co-immunoprecipitation assays. If it is confirmed that Ac78 does not interact with Ac92 in AcMNPV, then it is possible that Ac78 may interact with another protein located upstream or downstream in an oxidoreduction chain and the search for substrates of Ac92 sulfhydryl oxidation would continue.

The laboratory of Dr. Lorena Passarelli has already identified and produced constructs of additional late viral components that contain candidates that could potentially be substrates of Ac92. We could test whether the most promising of these potential substrates co-localize with Ac78 and Ac92 using the same methods described in Aim 1. In addition, we have a set of overlapping AcMNPV clones that represent the entire genome. These can be transfected singly or in combinations to determine if a specific region of the AcMNPV genome encodes a protein that co-localizes or co-immunoprecipitates with Ac92. The identification of an Ac78 interaction with another viral substrate would open the door for us to elucidate the biochemical mechanism of Ac78 with another substrate while still being in-line with the previous studies that show that deleting *ac78* results in a similar result as deleting *ac92*.

Additionally, our conclusion that an additional factor or factors resulting from AcMNPV infection is/are required for the localization of Ac92 to the nucleus warrants further investigation. Combinations of other late genes can be tested in our established immunofluorescence experiments in order to identify the specific factors necessary for the localization of Ac78 and Ac92 to the nucleus during viral infection.

The biochemical mechanisms underlying baculoviral capsid assembly are still largely undefined. Our characterization of the relationship between Ac78 and the AcMNPV sulfhydryl oxidase is a preliminary step in a broader effort to elucidate important biochemical pathways underlying the poorly described structural changes in capsid proteins and other proteins involved in virion stability, folding, and infectivity.

2.7 Significance

The study the mechanisms underlying baculoviral capsid assembly have immense ecological, agricultural, economic, and scientific importance. Baculoviruses play a critical ecological role in many ecosystems by naturally regulating insect populations (Podgwaite, et al., 1981; Bonsall, 2004; Myers & Cory, 2015) This observation from nature led baculoviruses to be harnessed as biological pesticides to protect agricultural crops. Baculoviruses have shown proven success at managing a number of infamous pest populations such as the larvae of *Galleria mellonella*, *Phthorimaea operculella*, *Spodoptera littorali*s, which destroy honey bee hives, potatoes, and cotton, respectively. Additionally, baculovirus-based pesticides have been applied to control Lepidoptera and Hymenoptera forest pests (Moscardi, 1999; Summers, 2006; Beek & Davis, 2016). Presently, there are thirteen NPV pesticide formulations against Lepidoptera and Coleoptera listed as approved for commercial use in the United States (Kalha et al., 2014; EPA, 2016). While a large need exists for effective and environmentally-friendly pesticides, widespread use of NPV-based pesticides has been limited by large-scale production challenges and efficacy of killing target pests in the field. One such barrier being addressed in other current studies is to increase the speed of action of the virus (i.e., alter how quickly AcMNPV kills its host and spreads to other insects) (Shim et al., 2013). Understanding the specific requirements necessary for the optimal function of the AcMNPV sulfhydryl oxidase (i.e. Ac92) and its potential cofactors (i.e., potentially Ac78) is relevant in ensuring optimal production of structural proteins necessary to increase the AcMNPV speed of action. Moreover, baculoviruses can be used as expression systems for proteins (Condreay et al., 2007) and vectors for gene delivery (Makkonen et al., 2015). Understanding capsid structure is relevant in developing ideal vectors tailored for gene delivery in the different biological environments of specific target tissues.

Describing the potential biochemical mechanisms of Ac78 and Ac92 could increase our understanding of the cofactors necessary for this viral sulfhydryl oxidase, which is vital to stabilizing the structures of many AcMNPV proteins and contributes to the overall structural properties of virions. Based on the high sequence conservation of Ac92, it is likely that key players in oxidoreductase pathways are similar in other baculoviral systems. Knowledge of the biochemical mechanisms of sulfhydryl oxidation in AcMNPV and the potential uses of this knowledge as explained above would likely be applied in other baculoviral systems. It is also possible that the conserved baculoviral sulfhydryl oxidase system could have similarities to other viral and cellular sulfhydryl oxidase systems yet to be discovered.

2.8 References

Akermann H.-W., Smirnoff W.A. (1983). A morphological investigation of 23 baculoviruses. J. Invertebr. Pathol. 41:269–280.

Condreay JP, Kost TA. (2007). Baculovirus expression vectors for insect and mammalian cells. Curr. Drug Targets 8:1126–1131

Federici, B.A. (1986). *Ultrastructure of baculoviruses,* in *The biology of baculoviruses,* R.R. Granados and B.A. Federici, Editors. CRC Press: Boca Raton. p. 61-88.

Fritz G, Roth A, Schiffer A, Büchert T, Bourenkov G, Bartunik HD, Huber H, Stetter KO, Kroneck PM, Ermler U. (2002). Structure of adenylylsulfate reductase from the hyperthermophilic Archaeoglobus fulgidus at 1.6-Å resolution. Proc. Natl. Acad. Sci. U. S. A. 99:1836–1841. http://dx.doi.org/10.1073/pnas.042664399.

Gabaldón T, Huynen MA. (2004). Prediction of protein function and pathways in the genome era. Cell. Mol. Life Sci. 61:930–944

Garavaglia MJ, Miele SAB, Iserte JA, Belaich MN, Ghiringhelli PD. (2012). The ac53, ac78, ac101, and ac103 genes are newly discovered core genes in the family Baculoviridae. J. Virol. 86:12069–12079. http://dx.doi.org/10.1128/JVI.01873-12.

Haase, S., Sciocco-Cap, A., & Romanowski, V. (2015). Baculovirus Insectides in Latin America: Historical Overview, Current Status, and Future Perspectives. *Viruses, 7*(5), 2230-2267.

Hakim M., et al. (2011). Structure of a Baculovirus Sulfhydryl Oxidase, A Highly Divergent Member of the Erv Flavoenzyme Family. *J Virol.* 85(18): 9406-9413

Javed, M. A., Biswas, S., Willis, L. G., Harris, S., Pritchard, C., Oers, M. M., . . . Theilmann, D. A. (2016). Autographa californica Multiple Nucleopolyhedrovirus AC83 is a Per Os Infectivity Factor (PIF) Protein Required for Occlusion-Derived Virus (ODV) and Budded Virus Nucleocapsid Assembly as well as Assembly of the PIF Complex in ODV Envelopes. *Journal of Virology,91*(5). doi:10.1128/jvi.02115-16

Kalha, C., Singh, P., Kang, S., Hunjan, M., Gupta, V., & Sharma, R. (2014). *Integrated Pest Management: Current Concepts and Ecological Management*. doi:https://doi.org/10.1016/B978-0-12-398529-3.00013-0

Kosugi S., Hasebe M., Tomita M., and Yanagawa H. (2009) Systematic identification of yeast cell cycle-dependent nucleocytoplasmic shuttling proteins by prediction of composite motifs. Proc. Natl. Acad. Sci. USA 106, 10171-10176.

Li, Sai-Nan, et al. (2014). Disruption of the baculovirus core gene ac78 results in decreased production of multiple nucleocapsid-Enveloped occlusion-derived virions and the failure of primary infection in vivo. *Virus Research,* vol. 191, pp. 70–82.

Long C.M., Rohrmann G.F., Merrill G.F. (2009). The conserved baculovirus protein p33 (Ac92) is a flavin adenine dinucleotide-linked sulfhydryl oxidase. *Virology.* 388(2): 231–5.

Martignoni, M. E., and P. J. Iwai. (1981). A catalogue of viral diseases of insects, mites, and ticks, p. 897-911. *In* H. D. Burges (ed.), Microbial control of pests and plant diseases 1970-1980. Academic Press, Inc., London, United Kingdom.

Mattevi A, Tedeschi G, Bacchella L, Coda A, Negri A, Ronchi S. (1999). Structure of L-aspartate oxidase: implications for the succinate dehydrogenase/fumarate reductase oxidoreductase family. Structure

Raychaudhuri A, Tipton PA. (2002). Cloning and expression of the gene for soybean hydroxyisourate hydrolase. Localization and implications for function and mechanism. Plant Physiol. 130:2061–2068. http://dx.doi.org/10.1104/pp.011049.

Rohrmann, G.F. (2008). *Baculovirus molecular biology.* Bethesda, MD: National Library of Medicine.

Shim, et al. (2013). NeuroBactrus, a Novel, Highly Effective, and Environmentally Friendly Recombinant Baculovirus Insecticide. *Applied and Environmental Microbiology*. 79: 141-149.

Tao, X. Y., et al. (2013). The Autographa californica Multiple Nucleopolyhedrovirus ORF78 Is Essential for Budded Virus Production and General Occlusion Body Formation. *Journal of Virology*, vol. 87, no. 15, pp. 8441–8450.

Vail P., et al. (1971). Recipocal infectivity of nuclear polyhedrosis viruses of the cabbage looper and alfalfa looper. *J Invertebr Pathol*. 17:383–388.

Wu, W., Clem, R. J., Rohrmann, G. F., & Passarelli, A. L. (2013). The baculovirus sulfhydryl oxidase Ac92 (P33) interacts with the Spodoptera frugiperda P53 protein and oxidizes it in vitro. *Virology,447*(1-2), 197-207. doi:10.1016/j.virol.2013.09.006

Wu W., Passarelli A.L. (2010). Autographa californica M nucleopolyhedrovirus Ac92 (ORF92, P33) is required for budded virus production and multiply-enveloped occlusion-derived virus formation. *J. Virol.* 84:12351–61.

2.9 Figures

Figure 2.1

A

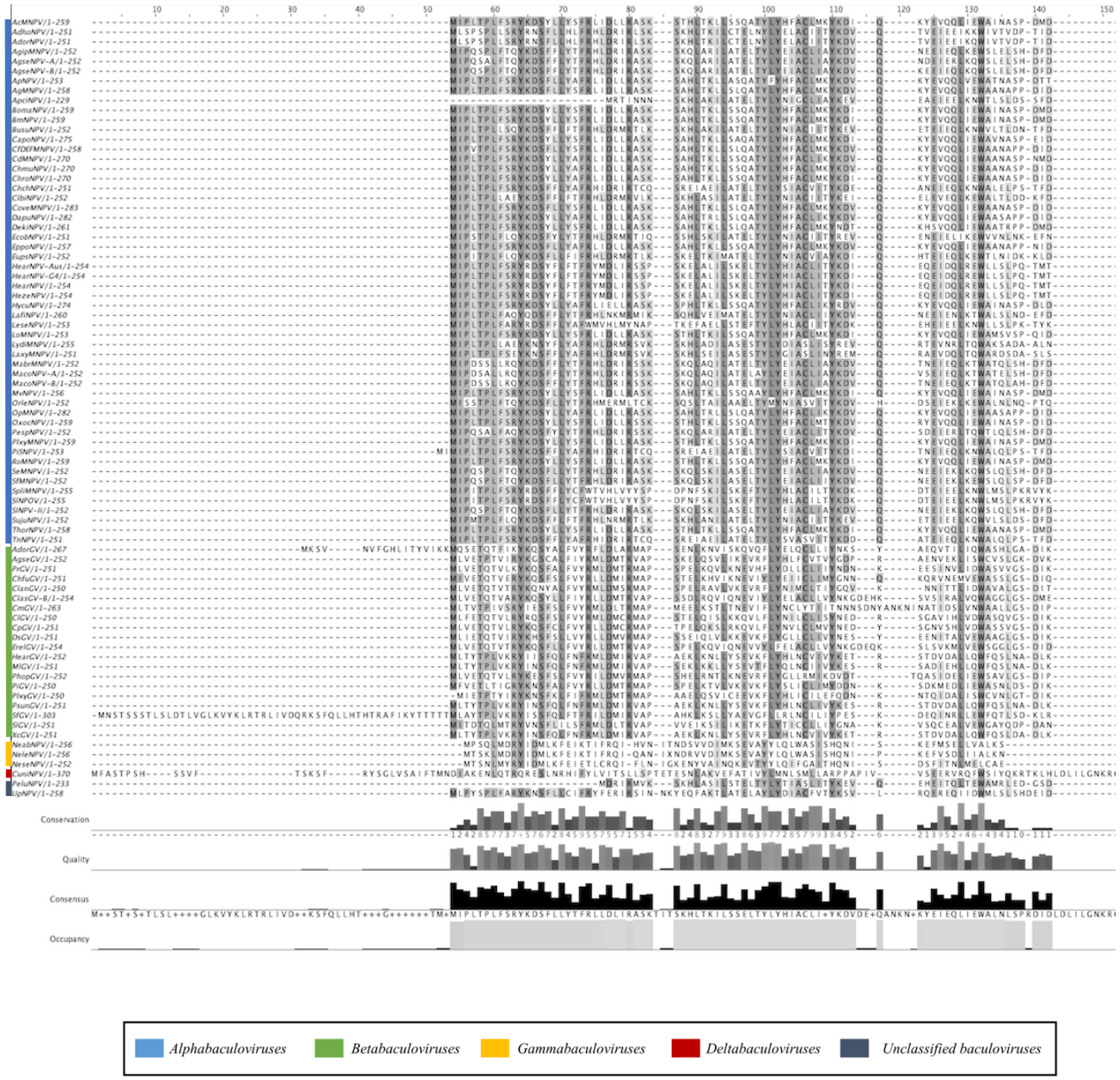
Conservation
Quality
Consensus
Occupancy
Alphabaculoviruses
Betabaculoviruses
Gammabaculoviruses
Deltabaculoviruses
Unclassified baculoviruses

Figure 2.1

B

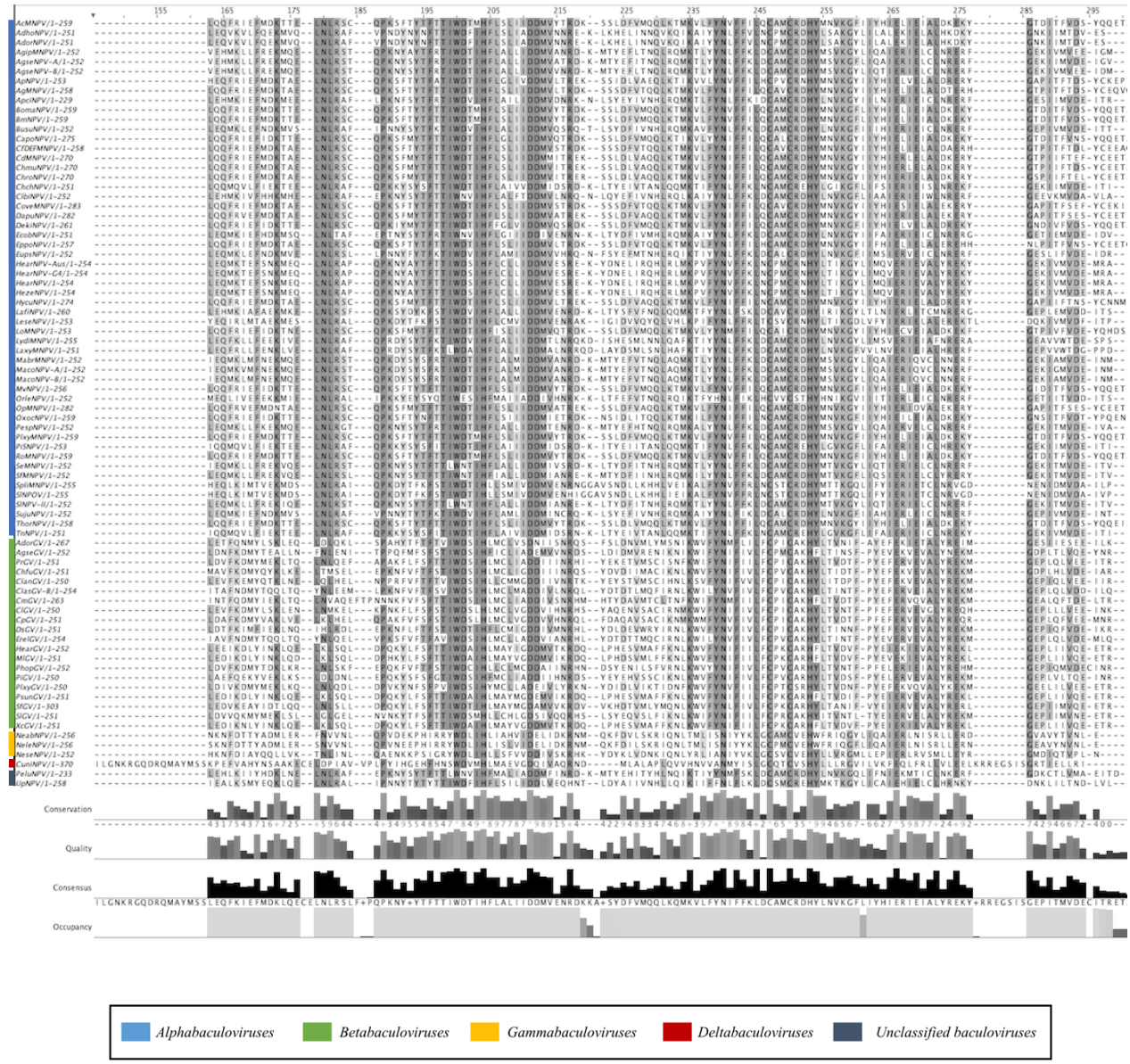
Conservation
Quality
Consensus
Occupancy
Alphabaculoviruses
Betabaculoviruses
Gammabaculoviruses
Deltabaculoviruses
Unclassified baculoviruses

Figure 2.1

C

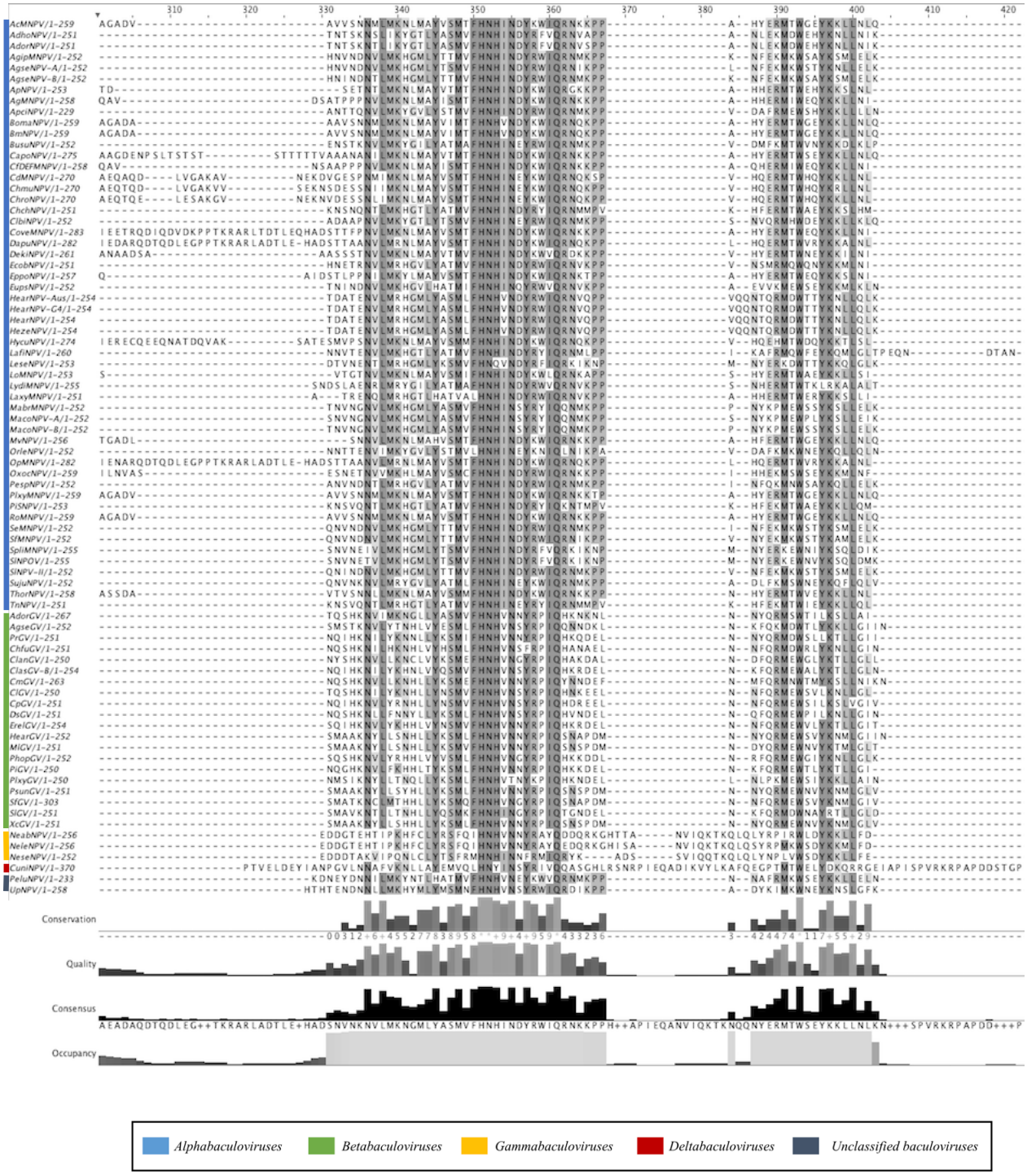
Conservation
Quality
Consensus
Occupancy
Alphabaculoviruses
Betabaculoviruses
Gammabaculoviruses
Deltabaculoviruses
Unclassified baculoviruses

Figure 2.1 Comprehensive multiple sequence alignment of 80 baculoviral FAD-linked sulfhydryl oxidases

Clustal Omega multiple alignment of 80 sequenced Ac92 homologs in baculoviruses. The AcMNPV Ac92 protein query sequence was used as the input to NCBI BLAST against the sequences of 79 of its homologs in other baculovirus species and strains. Amino acid sites that are highly conserved are shaded in the sequence alignment. Conservation is additionally shown graphically and numerically below each amino acid residue (for example, 3 = 30% conservation of the specific amino acid residue site, and + = 100% conservation). Below the conservation information, a quality score of the alignment is depicted graphically. A consensus of the most commonly-occurring amino acid residue at each site second from the bottom. The bottom row, "occupancy", graphically depicts sites at which any amino acid is present in all homologs.

(A) Multiple sequence alignment of the first 144 amino acids of Ac92 homologs.

(B) Multiple sequence alignment of amino acids 150-299 of Ac92 homologs.

(C)Multiple sequence alignment of amino acids 300-420 of Ac92 homologs.

Figure 2.2

A

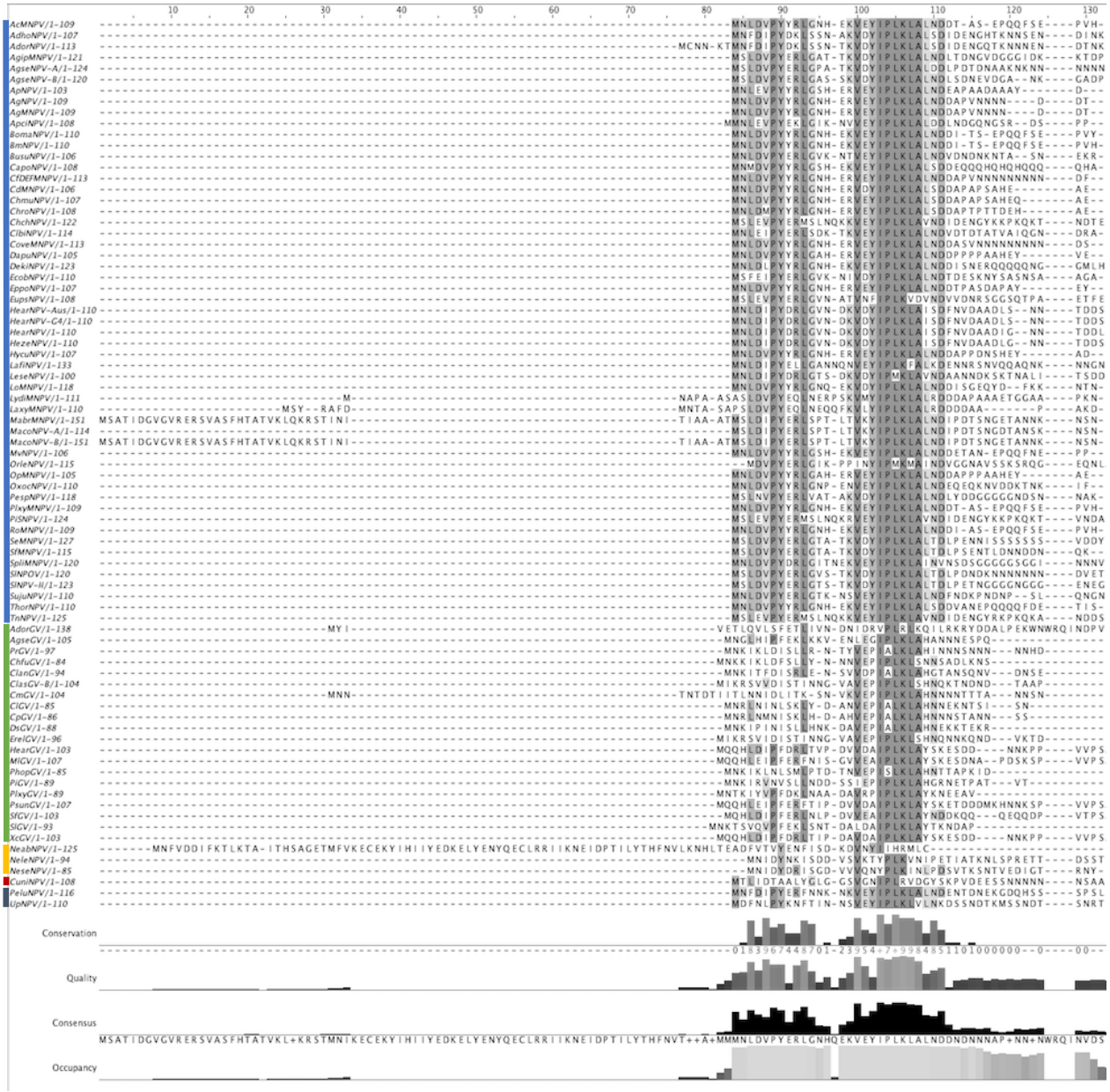
Conservation
Quality
Consensus
Occupancy
Alphabaculoviruses
Betabaculoviruses
Gammabaculoviruses
Deltabaculoviruses
Unclassified baculoviruses

B

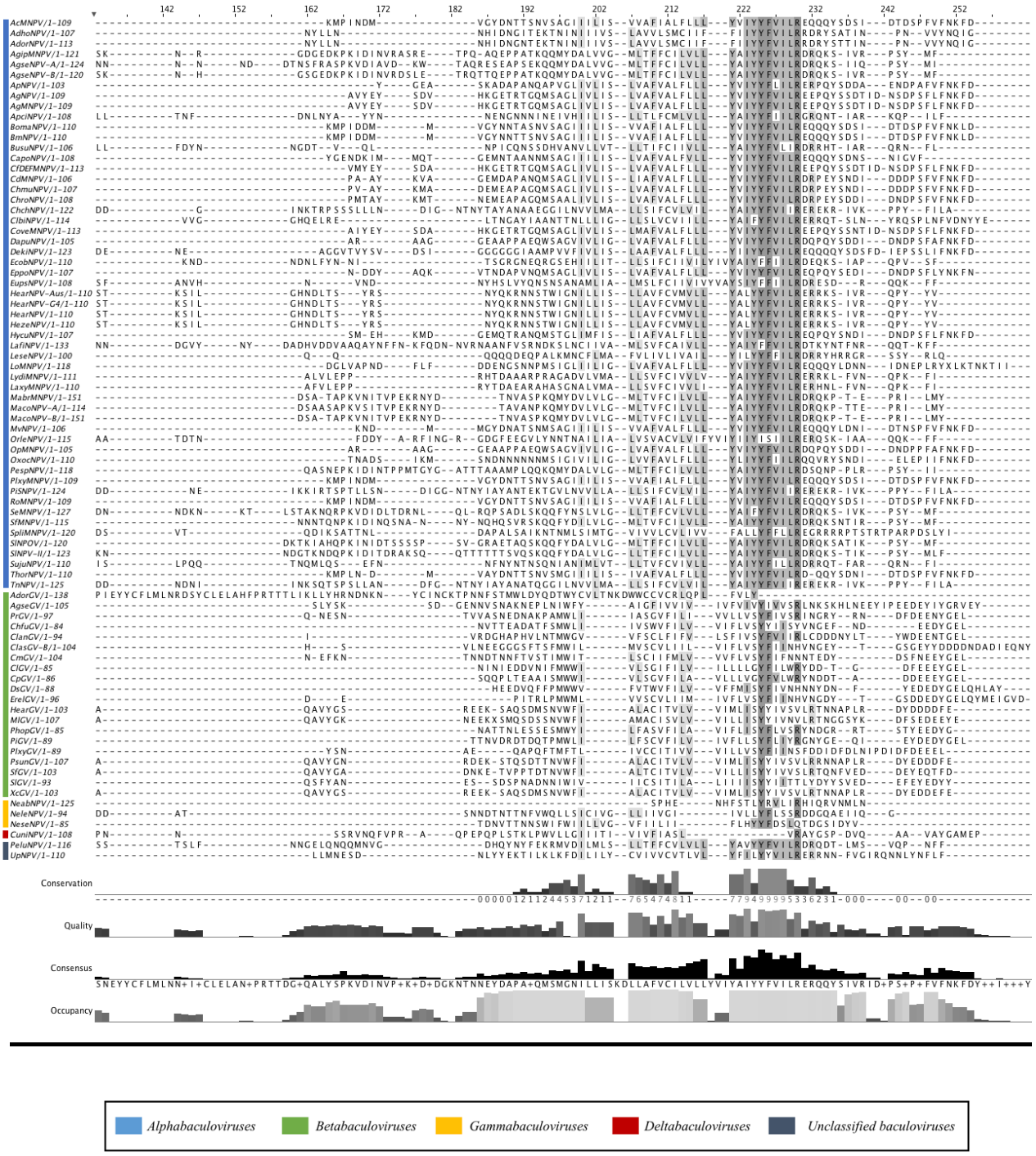
Conservation
Quality
Consensus
Occupancy
Alphabaculoviruses
Betabaculoviruses
Gammabaculoviruses
Deltabaculoviruses
Unclassified baculoviruses

Figure 2.2 Comprehensive sequence alignment of Ac78 homologs

Clustal Omega multiple alignment of 80 sequenced Ac78 homologs in baculoviruses. The AcMNPV Ac78 protein sequence was used as the input to NCBI BLAST against the sequences of 79 of its homologs in other baculovirus species and strains. Amino acid sites that are highly conserved are shaded in the sequence alignment. Conservation is additionally shown graphically and numerically below each amino acid residue site of the sequence alignment (for example, 3 = 30% conservation of the specific amino acid residue site, and + = 100% conservation). Below the conservation information, a quality score of the alignment is depicted graphically. A consensus of the most commonly-occurring amino acid residue at each site second from the bottom. The bottom row, “occupancy”, graphically depicts sites at which any amino acid is present in all homologs.

(A) Multiple sequence alignment of the first 132 amino acids of Ac78 homologs. The highly conserved IPLKL motif is located from amino acid residues 101-108 of the multiple sequence alignment. Additionally, Ac78 and its homologs contain a transmembrane motif (sites 61-83 of AcMNPV Ac78), despite a lack of conservation of specific amino acid residues at this site.

(B) Multiple sequence alignment of amino acids 130-255 of Ac78 homologs. The FRF C-terminal motif is located between amino acid residue sites 187-254 of this multiple sequence alignment.

Figure 2.3

Ac92

```
MIPLTPLFSRYKDSYLLYSFRLIDLLRASKSTHLTKLLSSQATYLYHFAC 50
LMKYKDIQKYEVQQLIEWAINASPDMDLQQFRIEFMDKTTELNLRSCQPK 100
SFTYTFTTIWDTMHFLSLIIDDMVYTRDKSSLDFVMQQLKTMKVLFYNVF 150
FILQCAMCRDHYMNVKGFIIYHIELIEIALDKEKYGTDITFVDSYQQETA 200
GADVAVVSNNMLMKNLMAYVSMTFHNHINDYKWIQRNKKPPAHYERMTWG 250
EYKKLLNLQ                                          259
```

Ac78

```
MNLDVPYYRLGNHEKVEYIPLKLALNDDTASEPQQFSEPVHKMPINDMVG 50
YDNTTSNVSAGIIILISVVAFIALFLLLYVIYYFVILREQQQYSDSIDTD 100
SPFVFNKFD                                          109
```

Figure 2.3 - Ac78 and Ac92 predict nuclear and cytoplasmic localization regions

The Ac92 protein query sequence (A) or Ac78 protein query sequence (B) was entered into cNLS Mapper software, which predicts nuclear localization sequences (NLSs) specific to the importin α/β pathway by calculating NLS scores with four NLS categories. The NLS categories were generated using extensive amino acid replacement analysis in budding yeast to give positive or negative contribution scores to each amino acid residue, which contributes to the overall nuclear localization activity of the sequence. Because the importin α/β nuclear import pathway is highly conserved among eukaryotes, the prediction of the cNLS mapper based on yeast may still yield valuable information but may not be as effective in other species. Ac92 and Ac78 contained predicted NLS sequences with scores of 3.6 and 3.7, respectively. A GUS-GFP reporter protein fused to an NLS with a score of 3-5 localized to both the nucleus and the cytoplasm. Thus, both Ac78 and Ac92 contained sequences predicted by the cNLS mapper to have both cytoplasmic and nuclear localization.

Figure 2.4

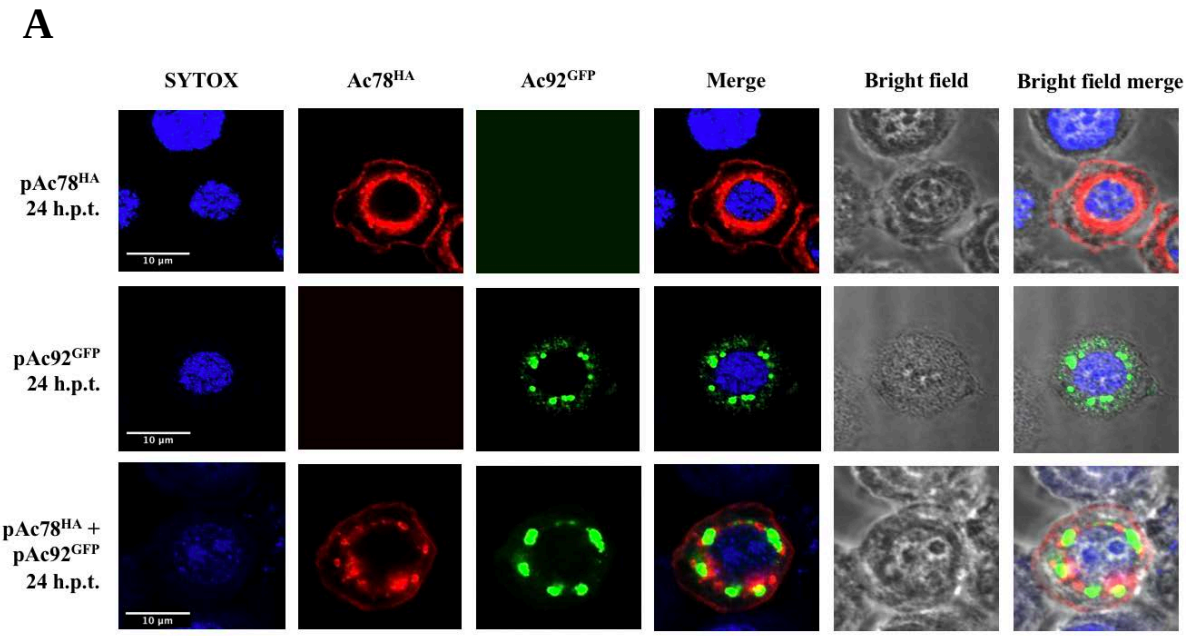
A
SYTOX
Ac78HA
Ac92GFP
Merge
Bright field
Bright field merge
pAc78HA 24 h.p.t.
pAc92GFP 24 h.p.t.
pAc78HA + pAc92GFP 24 h.p.t.
10 µm
10 µm
10 µm

Figure 2.4

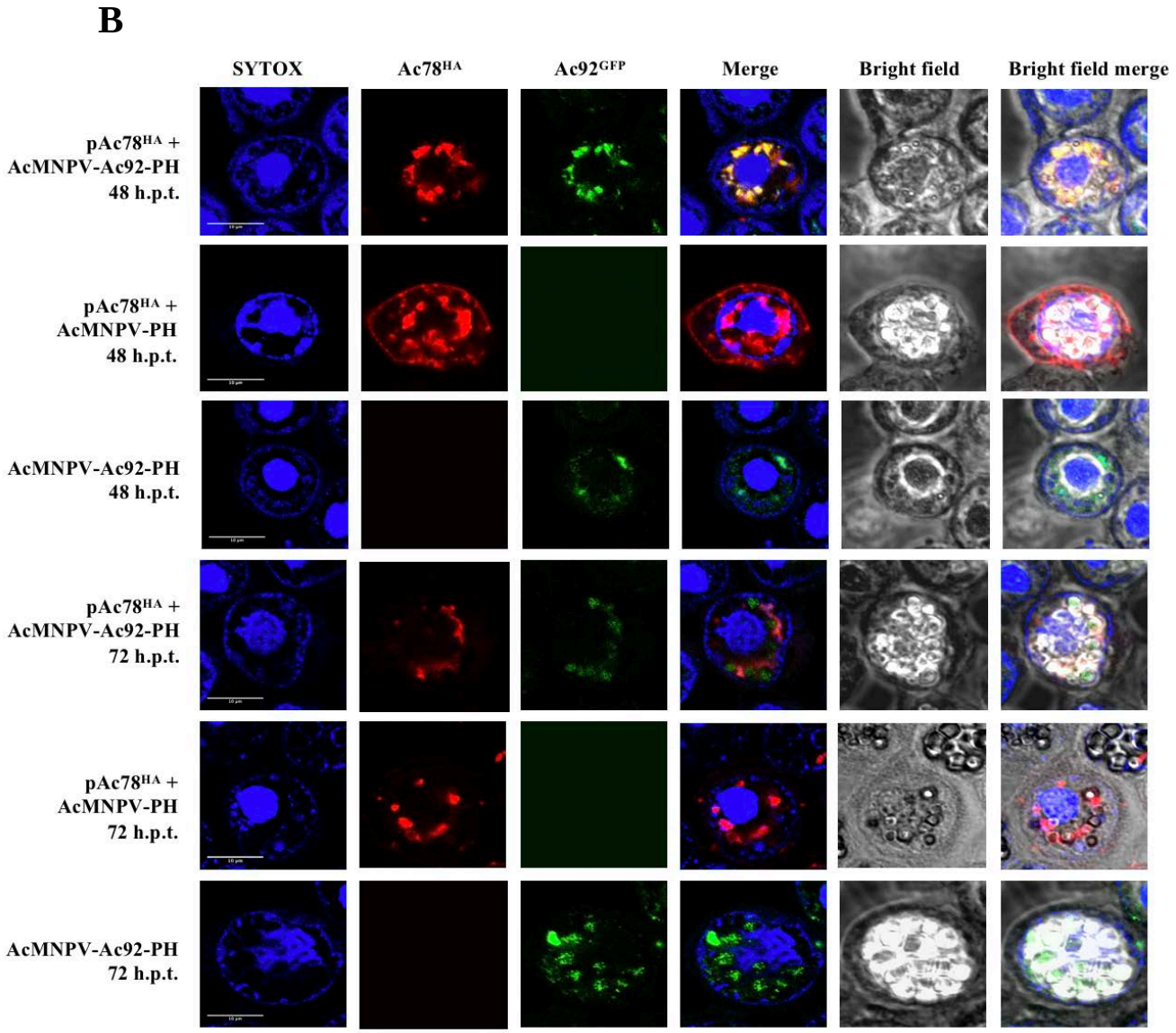
B
SYTOX
Ac78HA
Ac92GFP
Merge
Bright field
Bright field merge
pAc78HA + AcMNPV-Ac92-PH 48 h.p.t.
pAc78HA + AcMNPV-PH 48 h.p.t.
AcMNPV-Ac92-PH 48 h.p.t.
pAc78HA + AcMNPV-Ac92-PH 72 h.p.t.
pAc78HA + AcMNPV-PH 72 h.p.t.
AcMNPV-Ac92-PH 72 h.p.t.

Figure 2.4

C

Sample	Percent of cells in which Ac78 localized perinuclearly in cytoplasm in evenly-distributed fashion	Percent of cells in which Ac78 was found on plasma membrane	Percent of cells in which Ac92 localized perinuclearly in cytoplasm in punctate fashion
pAc78-HA 24 h.p.t.	60.9% (n=69)	89.9% (n=69)	00.0% (n=69)
pAc92-GFP 24 h.p.t.	00.0% (n=77)	00.0% (n=77)	79.2% (n=77)
pAc78-HA + pAc92-GFP 24 h.p.t.	62.5% (n=48)	93.8% (n=48)	70.8% (n=48)

Sample	Percent of cells in which Ac78 localized in intranuclear ring zone	Percent of cells in which Ac78 was found on plasma membrane	Percent of cells in which Ac92 localized in intranuclear ring zone
pAc78-HA + vAc92-GFP 48 h.p.t.	96.0% (n=50)	32.0% (n=50)	92.0% (n=50)
pAc78-HA + AcMNPV 48 h.p.t.	100.0% (n=31)	83.9% (n=31)	NA
vAc92-GFP 48 h.p.t.	00.0% (n=45)	00.0% (n=45)	100% (n=45)
pAc78-HA + vAc92-GFP 72 h.p.t.	100.0% (n=44)	18.2% (n=44)	100% (n=44)
pAc78-HA + AcMNPV 72 h.p.t.	100.0% (n=57)	28.1% (n=57)	NA
vAc92-GFP 48 h.p.t.	00.0% (n=58)	00.0% (n=58)	100.0% (n=58)

Figure 2.4 - Localization of Ac78 and Ac92 in the presence and absence of AcMNPV infection

Localization of Ac92 and Ac78 by immunofluorescence staining. Sf9 cells were transfected with the indicated viral (AcMNPV-Ac92-PH) or plasmid (pAc78^{HA} or pAc92^{GFP}) DNA, and Ac92 and Ac78 localization were examined by confocal microscopy. SYTOX Orange was used to stain nuclei of the cells (blue). Ac78 was detected by anti-HA antisera (red). Ac92 contained a GFP fusion tag.

(A) Ac92 localization was not affected by Ac78. Ac92 was expressed as a C-terminal EGFP fusion under hsp70 promoter, and its localization detected by visualizing GFP (green).

(B) Localization of Ac92 and Ac78 in the presence of baculovirus infection. Ac92 was expressed as a C-terminal EGFP fusion in a polyhedrin+ AcMNPV, and its localization was detected by visualizing GFP (green). The merge shows a merge of the SYTOX Orange, Ac78HA, and Ac92GFP images. The bright field merge includes the bright field image in the merged images. Arrows indicate occlusion bodies in the nucleus of infected cells.

(C) The images shown in parts (A) and (B) of this report were representative of the majority of cells analyzed. The percent of analyzed cells for which the indicated observations were observed are recorded in (C). A minimum of 2 biological replicates were performed for each condition.

Figure 2.5

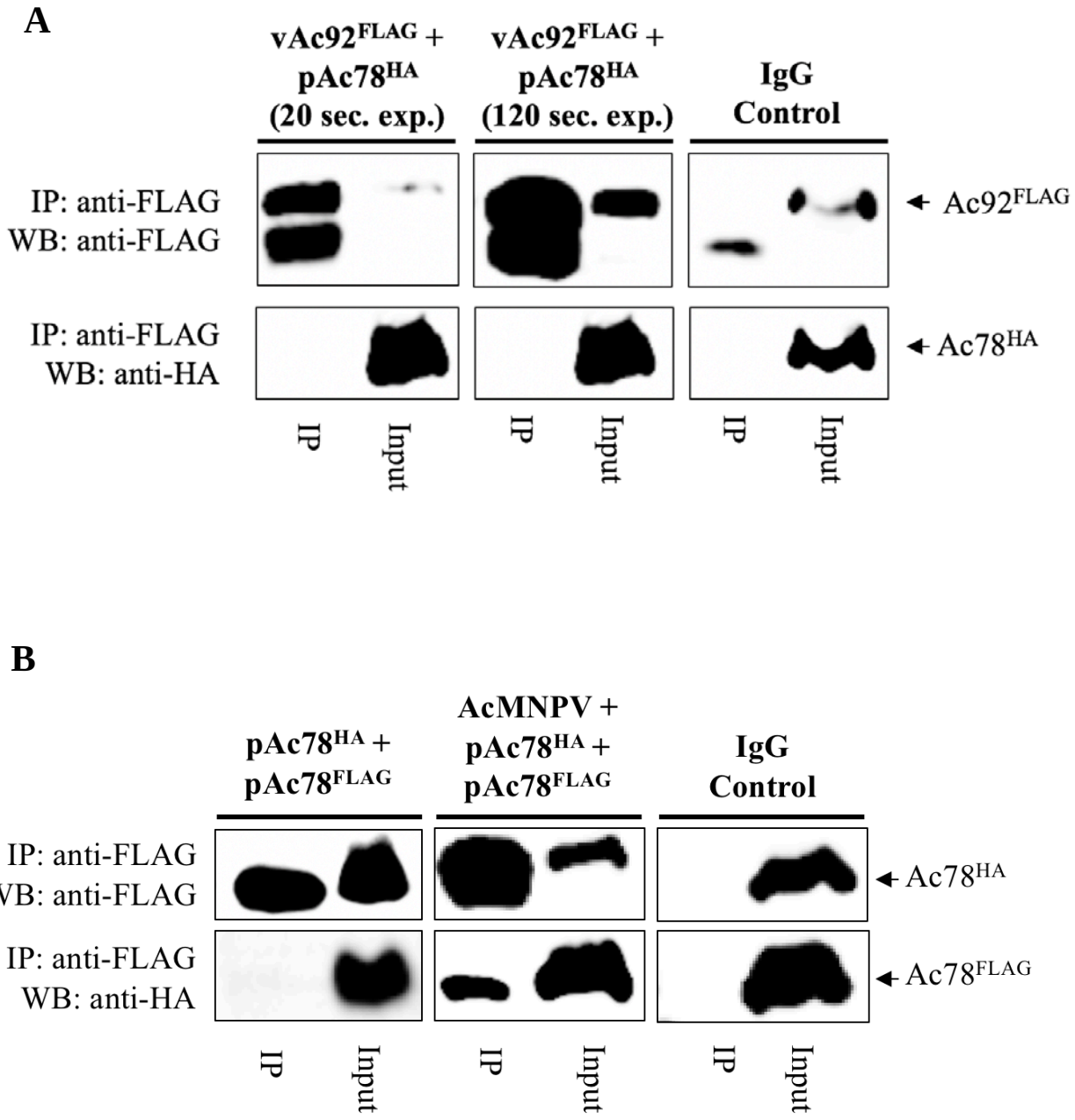
A
vAc92FLAG + pAc78HA (20 sec. exp.)
vAc92FLAG + pAc78HA (120 sec. exp.)
IgG Control
IP: anti-FLAG WB: anti-FLAG
IP: anti-FLAG WB: anti-HA
Ac92FLAG
Ac78HA
IP
Input
B
pAc78HA + pAc78FLAG
AcMNPV + pAc78HA + pAc78FLAG
IgG Control
IP: anti-FLAG WB: anti-FLAG
IP: anti-FLAG WB: anti-HA
Ac78HA
Ac78FLAG
IP
Input

Figure 2.5 - Co-immunoprecipitation of Ac78 and Ac92

Sf9 cells were cotransfected with the indicated plasmids (pAc78HA, pAc78FLAG) or infected with the indicated virus (vAc92FLAG or AcMNPV) as indicated above each lane. At 24 h p.t. or 48 h p.i., cells were collected and lysed for immunoprecipitation using the antibodies indicated as “IP” to the left. Transferred proteins were probed with the antibodies indicated as “WB” to the left. Input = input cell lysates; IgG control = control immunoprecipitation with mouse IgG; IP = immunoprecipitation with the antibody indicated to the left. Plasmid names: pAc78HA = phsp70-Ac78HA; pAc78FLAG = phsp70-Ac78FLAG. Virus names: AcMNPV = wildtype AcMNPV L1 strain; vAc92FLAG = rescue virus containing GFP and C-terminally-tagged Ac92-FLAG.

(A) Co-immunoprecipitation of pAc78HA with vAc92FLAG

(B) Co-immunoprecipitation of Ac78HA and Ac78FLAG in the presence or absence of other AcMNPV proteins.

Figure 2.6

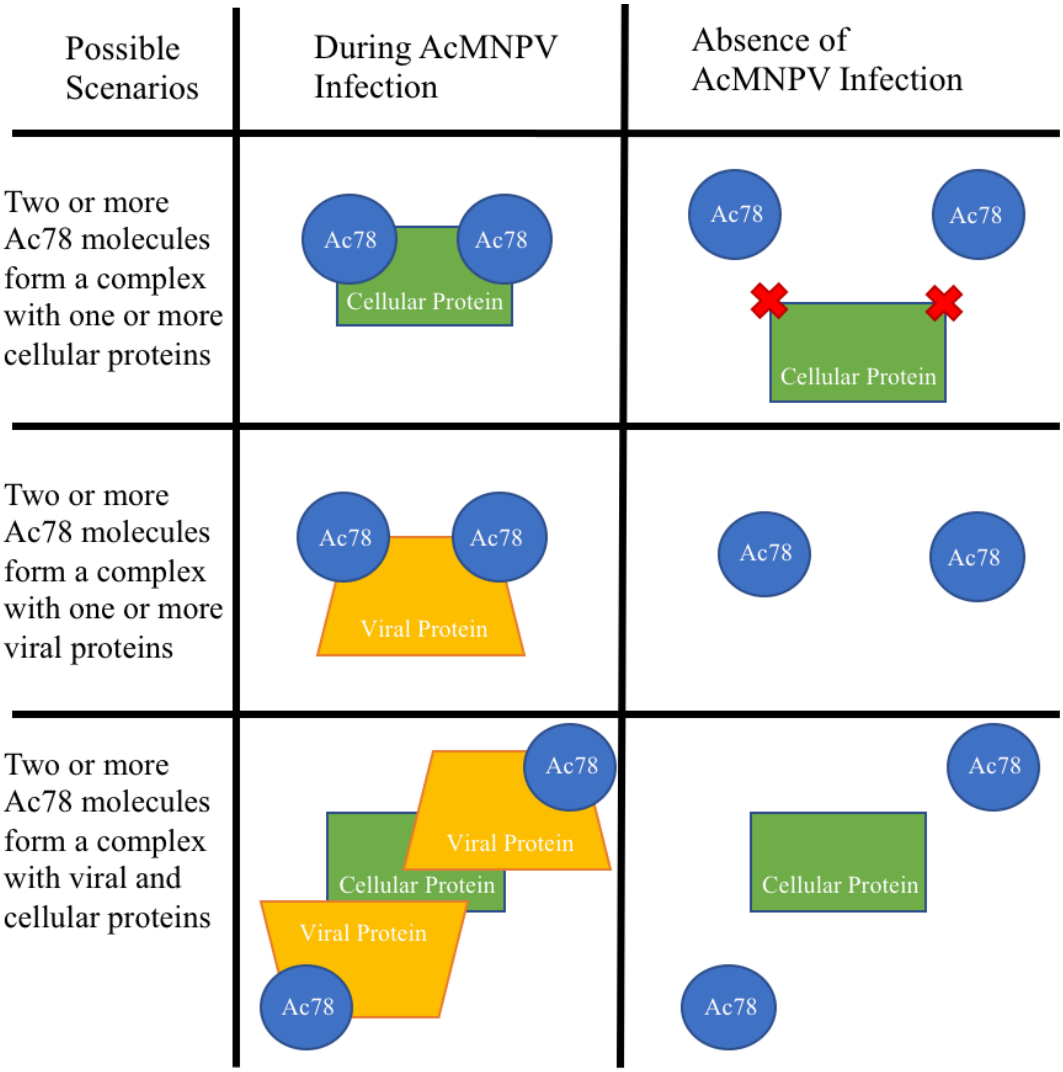
Possible Scenarios
During AcMNPV Infection
Absence of AcMNPV Infection
Two or more Ac78 molecules form a complex with one or more cellular proteins
Ac78
Ac78
Cellular Protein
Ac78
Ac78
Cellular Protein
Two or more Ac78 molecules form a complex with one or more viral proteins
Ac78
Ac78
Viral Protein
Ac78
Ac78
Two or more Ac78 molecules form a complex with viral and cellular proteins
Ac78
Viral Protein
Cellular Protein
Viral Protein
Ac78
Ac78
Cellular Protein
Ac78

Figure 2.6 - Possible models of Ac78 physical interaction

The result that at least two differentially-tagged Ac78 molecules associated during AcMNPV infection but not in the absence of other AcMNPV proteins indicates that one of several possibilities may have occurred. One possibility is that Ac78 complexed with a cellular protein that was modulated during AcMNPV infection. For example, a cellular protein could have experienced a conformational change such as phosphorylation or methylation by an AcMNPV protein during infection that allowed for its association with Ac78. Alternatively, expression of the cellular protein may have been upregulated during AcMNPV infection. A second possibility is that Ac78 associates with other AcMNPV protein(s). A third possibility is that Ac78 associates with a complex of other viral and cellular proteins that does not form in the absence of AcMNPV infection.

2.10 Tables

Table 2.1

Virus abbreviation	Virus name
AcMNPV	Autographa californica nucleopolyhedrovirus
AdhoNPV	Adoxophyes honmai nucleopolyhedrovirus
AdorNPV	Adoxophyes orana nucleopolyhedrovirus
AgipMNPV	Agrotis ipsilon multiple nucleopolyhedrovirus
AgseNPV-A	Agrotis segetum nucleopolyhedrovirus A
AgseNPV-B	Agrotis segetum nucleopolyhedrovirus B
ApNPV	Antheraea pernyi nucleopolyhedrovirus
AgMNPV	Anticarsia gemmatalis multiple nucleopolyhedrovirus
ApciNPV	Apocheima cinerarium nucleopolyhedrovirus
BomaNPV	Bombyx mandarina nucleopolyhedrovirus
BmNPV	Bombyx mori nucleopolyhedrovirus
BusuNPV	Buzura suppressaria nucleopolyhedrovirus
CapoNPV	Catopsilia pomona nucleopolyhedrovirus
CfDEFMNPV	Choristoneura fumiferana DEF multiple nucleopolyhedrovirus
CdMNPV	Choristoneura fumiferana multiple nucleopolyhedrovirus
ChmuNPV	Choristoneura murinana nucleopolyhedrovirus
ChroNPV	Choristoneura rosaceana nucleopolyhedrovirus

Virus abbreviation	Virus name
ChchNPV	Chrysodeixis chalcites nucleopolyhedrovirus
ClbiNPV	Clanis bilineata nucleopolyhedrovirus
CoveMNPV	Condylorrhiza vestigialis MNPV
DapuNPV	Dasychira pudibunda nucleopolyhedrovirus
DekiNPV	Dendrolimus kikuchii nucleopolyhedrovirus
EcobNPV	Ectropis obliqua nucleopolyhedrovirus
EppoNPV	Epiphyas postvittana nucleopolyhedrovirus
EupsNPV	Euproctis pseudoconspersa nucleopolyhedrovirus
HearNPV-Aus	Helicoverpa armigera nucleopolyhedrovirus strain Australia
HearNPV-G4	Helicoverpa armigera nucleopolyhedrovirus G4
HearNPV	Helicoverpa armigera nucleopolyhedrovirus
HezeNPV	Helicoverpa zea single nucleopolyhedrovirus
HycuNPV	Hyphantria cunea nucleopolyhedrovirus
LafiNPV	Lambdina fiscellaria nucleopolyhedrovirus
LeseNPV	Leucania separata nucleopolyhedrovirus
LoMNPV	Lonomia obliqua multiple nucleopolyhedrovirus
LaxyMNPV	Lymantria xylina nucleopolyhedrovirus

Virus abbreviation	Virus name
LydiMNPV	Lymantria dispar multiple nucleopolyhedrovirus
MabrMNPV	Mamestra brassicae multiple nucleopolyhedrovirus
MacoNPV-A	Mamestra configurata nucleopolyhedrovirus A
MacoNPV-B	Mamestra configurata nucleopolyhedrovirus B
MvNPV	Maruca vitrata nucleopolyhedrovirus
OrleNPV	Orgyia leucostigma nucleopolyhedrovirus
OpMNPV	Orgyia pseudotsugata multiple nucleopolyhedrovirus
OxocNPV	Oxyplax ochracea nucleopolyhedrovirus
PespNPV	Peridroma alphabaculovirus
PlxyMNPV	Plutella xylostella multiple nucleopolyhedrovirus
PiSNPV	Pseudoplusia includens SNPV IE
RoMNPV	Rachiplusia ou MNPV
SeMNPV	Spodoptera exigua multiple nucleopolyhedrovirus
SfMNPV	Spodoptera frugiperda multiple nucleopolyhedrovirus
SpliMNPV	Spodoptera littoralis nucleopolyhedrovirus
SlNPV	Spodoptera litura nucleopolyhedrovirus
SlNPV-II	Spodoptera litura nucleopolyhedrovirus II
SujuNPV	Sucra jujuba nucleopolyhedrovirus
ThorNPV	Thysanoplusia orichalcea nucleopolyhedrovirus

Virus abbreviation	Virus name
TnNPV	Trichoplusia ni single nucleopolyhedrovirus
AdorGV	Adoxophyes orana granulovirus
AgseGV	Agrotis segetum granulovirus
PrGV	Pieris rapae granulovirus
ChfuGV	Choristoneura fumiferana granulovirus
ClanGV	Clostera anachoreta granulovirus
ClasGV-B	Clostera anastomosis granulovirus B
CmGV	Cnaphalocrocis medinalis granulovirus
ClGV	Cryptophlebia leucotreta granulovirus
CpGV	Cydia pomonella granulovirus
DsGV	Diatraea saccharalis granulovirus
ErelGV	Erinnyis ello granulovirus
HearGV	Helicoverpa armigera granulovirus
MlGV	Mocis latipes granulovirus
PhopGV	Phthorimaea operculella granulovirus
PiGV	Plodia interpunctella granulovirus
PlxyGV	Plutella xylostella granulovirus
PsunGV	Pseudalatia unipuncta granulovirus
SfGV	Spodoptera frugiperda granulovirus
SlGV	Spodoptera litura granulovirus
TnNPV	Trichoplusia ni single nucleopolyhedrovirus

Virus abbreviation	**Virus name**
XcGV	Xestia c-nigrum granulovirus
NeabNPV	Neodiprion abietis nucleopolyhedrovirus
NeleNPV	Neodiprion lecontei nucleopolyhedrovirus
NeseNPV	Neodiprion sertifer nucleopolyhedrovirus
CuniNPV	Culex nigripalpus nucleopolyhedrovirus
PeluNPV	Perigonia lusca single nucleopolyhedrovirus
UpNPV	Urbanus proteus nucleopolyhedrovirus

Table 2.1 – Table of baculovirus abbreviations used in Figures 2.1 and 2.2

Chapter 3 - Interaction of C protein with the measles virus replication complex

3.1 Introduction

3.1.1 An overview of measles virus

Measles virus (MeV) is human-specific pathogen belonging to the *Morbilivirus* genus, *Paramyxovirinae* subfamily, *Paramyxoviridae* family, and *Mononegavirales* order (ICTV, 2017). MeV and other closely related viruses are actively being researched due to their significant impacts as pathogens of humans and economically important livestock and pets. For example, rinderpest virus, another *Morbilivirus* and causative agent of a highly fatal disease in even-toed ungulates, threatened the human food supply since the origin of herding but became the second pathogen in history to be eradicated in 2011 (World Health Organization, 2011). Canine distemper virus, which causes a lethal disease in the respiratory system of puppies and dogs and threatens pets of the some 48% of U.S. households that own canines, recently expanded its host range into nonhuman primates (APPA, 2017; Sakai, 2013). MeV has infected humans for millennia and is the causative agent of the disease called measles. The first century Persian physician Rhazes first demarcated Measles from other diseases in *"A Treatise Smallpox and Measles" (*Rāzī & Greenhill, 1847). Measles has the potential to be lethal and includes symptoms of rash, malaise, anorexia, coryzva, and conjunctivitis. Prior to the development of the Edmonston-strain MeV attenuated vaccine in 1963, a vast majority of humans contracted MeV during childhood (Hendriks & Blume, 2013). It is reported that 97% of people who receive two doses containing MeV-Edm are protected from Measles, and vaccination strategies against MeV

have been highly effective when implemented properly (CDC, 2017). Although MeV is capable of entering the cells of humans, nonhuman primates, and some rodents, an active infection can only be established in humans (Zhu et al., 1997; Van et al., 1995). Because there are no other known reservoirs of MeV, MeV is an ideal target for eradication (WHO, 2006). In addition to serving as a vaccine against wild type MeV, vaccine-strain MeVs have oncolytic tendencies in some human cancers and are active subjects of numerous clinical trials (Msaouel et al., 2018). Like all other members of *Mononegavirales*, MeV contains a negative-sense, single-stranded RNA genome. The MeV genome is non-segmented, 15,894 nucleotides (nt) in length, and encodes six individual genes that encode eight protein products: 1. nucleoprotein (N), 2. phosphoprotein (P), V protein, and C protein, 3. matrix protein (M), 4. fusion protein (F), 5. hemagglutinin (H), and 6. large RNP-dependent RNA polymerase (L) (Figure 3.1A; Lamb & Parks, 2013; Griffin, 2013; Horikami, 1995). MeV enters cells of the immune, epithelial, and respiratory systems via binding of H to specific receptors: signaling activation lymphocyte molecule (SLAM) expressed on immune cells, CD46 expressed on epithelia, and Nectin-4. Upon binding to the receptor, H undergoes a conformational change that allows F to trigger fusion between the virion and cell membranes (Malvoisin and Wild, 1993). In the cytoplasm, L and P serve functions involved in the replication of the MeV genome, which is encapsidated by N. During assembly of new viral particles, M functions in the assembly of new MeV particles by linking ribonucleoproteins with envelope proteins. C and V are encoded by alternative open reading frames of the P gene and have known functions in modulation of the host innate immune defense (Audsley & Moseley, 2013; Parks & Alexander-Miller, 2013; Chambers & Takimoto, 2009).

3.1.2 Measles virus replication complex and C protein

MeV replication occurs in the cytoplasm of infected cells. The ribonucleoprotein (RNP)-dependent RNA polymerase complex consists of the catalytic subunit, L, which interacts with its cofactor, P. The template consists of a viral negative-sense genomic RNA encapsidated by N, which together form a helical RNP structure. Replication begins at the 3' end of the template, where the replication complex associates with the template and P interacts with N (Figure 3.1C). The product of replication is a complementary nascent RNA, which is co-transcriptionally encapsidated with N (Longhi, 2009). The MeV replication complex is able to use both genomic or antigenomic RNA as a template for replication. Genomic (negative-sense) RNA serves as a template for the generation of full-length antigenomic (positive-sense) RNA strands and capped and polyadenylated mRNAs. Processed mRNAs can then be translated into protein using the host translational machinery, and full-length positive-sense antigenomic RNAs can be used as the templates for generating new negative-sense genomes (Rima & Duprex, 2009).

Replication by the MeV replication complex is error-prone and occasionally defective genomes are produced. The laboratory of Dr. Roberto Cattaneo previously showed that MeV-Edm and wild-type MeV (MeV-wt) strains lacking C generated 10 times more 5′ copy-back defective interfering RNAs (DI-RNAs), which are potent inducers of innate immune response including induction of PKR and interferon (IFN) (Pfaller et al., 2014; Holland et al., 1980). Additionally, there is evidence that C requires L to localize to the site of viral infection with the known components of the MeV replication complex: N, P, and L (Cattaneo Lab unpublished data; Ito et al., 2013). These observations suggest that C may function as a quality control factor in MeV replication by serving as a stabilizing component of members of the replication complex. However, a mechanism by which C may interact with the MeV replication complex has yet to be

shown. In order to gain insight into the biochemical mechanism by which C is involved in MeV replication, we performed co-immunoprecipitation experiments between C and N, P, and L. Co-immunoprecipitation experiments showed that during MeV infection, C associated with large protein (L) and phosphoprotein (P), which comprise the MeV replication complex, and nucleoprotein (N), which encapsidates the RNA genome. Expression constructs for full-length MeV L were generated, and L was successfully expressed following transfection. Subsequent co-immunoprecipitation experiments showed that C did not precipitate with L, P, nor N when transfected in isolation from MeV infection, indicating that another factor resulting from MeV infection is necessary for the association of C with the MeV replication complex. The results of this investigation are an important step in elucidating a biochemical mechanism underlying the function of C as a quality control factor in MeV replication. MeV has been attenuated and is a highly effective vaccine against pathogenic MeV and an active subject of clinical research as an oncolytic agent for treating a number of human cancers.

3.2 Materials and methods

Virus and cells

A MeV containing FLAG-tagged C and HA-tagged L (MeV-vac2-2tags) was generated using methods as recently described (Ma et al., 2018). Briefly, the Moraten vaccine strain MeV (MeV-vac2) (Pfaller et al. 2015) was modified by the knockout of endogenous C from the P/V/C gene, insertion of a gene encoding FLAG-tagged C between H and L genes, and the addition of an HA tag to the L gene (Figure 3.1B).

The 293T cells used in all transfection experiments are from clone 293T/17 purchased from ATCC (catalog number CRL-11268).

Plasmid cloning

Expression constructs for full-length L with an HA tag at the N-terminus (pCAGGS-^{HA}L) and a full-length L with an HA tag at the C-terminus (pCAGGS-L^{HA}) were cloned into the pCAGGS vector provided by Friedemann Weber (described in Niwa et al., 1991). The ^{HA}L insert for pCAGGS-^{HA}L was PCR-amplified from pCG-^{HA}L plasmid using a forward primer containing NotI (5'- ATCTGGCGGCCGCGCCACCATGTACCCATACGATGTTCCAG -3') and reverse primer containing BamHI (5'-GATCG GGATCC TTAGTCCTTAATCAGGGCACTG-3'). The L^{HA} insert for pCAGGS-L^{HA} was PCR-amplified from the pCG-L^{HA} plasmid using a forward primer containing NotI (5'-ATCTGGCGGCCGCGCCACCATGGACTCGCTATCTGTCAAC-3') and a reverse primer containing BamHI (5'-GATCGGGATCCTTAAGCGTAATCTGGAACATC-3'). The respective PCR products were purified (PCR purification kit; Qiagen, Valencia, CA), digested with NotI and BamHI (New England BioLabs, Ipswich, MA), purified again, and then ligated with the NotI/BamHI-linearized pCAGGS vector. Ligation products were transformed into OneShot TOP10 cells (Life Technologies, Carlsbad, CA), and the bacteria were plated on LB-ampicillin agar plates and incubated at 37°C for 14 to 20 hours. Single colonies were picked and resuspended in 10 µl H_2O, and 5 µl of the suspension was subjected to colony PCR using a forward primer, which binds to the backbone upstream of the L insert (5'-TACAGCTCCTGGGCAACG-3') and a reverse primer which binds within the L open reading frame (5'-CTGTAAGCGTGAGGGAC-3') and a 2X PCR master mix (Promega, Madison, WI). Clones with individual inserts, as analyzed by 1% agarose

gel electrophoresis, were selected and grown in 2 ml LB-ampicillin, and plasmids were extracted using a plasmid minikit (Qiagen,Valencia, CA). Sequences were determined by Sanger sequencing using the same forward primer which binds to the backbone upstream of L (5'-TACAGCTCCTGGGCAACG-3') and a reverse primer which binds to the backbone downstream of the L insert (5'-GCCAGAAGTCAGATGCTC-3').

An expression construct encoding FLAG-tagged C (pCAGGS C^{FLAG}) was cloned into the pCAGGS vector. The C^{FLAG} insert sequence was amplified from the pCR3-C^{FLAG} template using a forward primer containing NotI restriction site (5'-ATCTGGCGGCCGCGCCACCATGCATAGGAGGCACCTTGTGG-3') and a reverse primer containing BamHI restriction site (5'-CGATCGGATCCTTAGCTCTGGGTGTATAGCCTTG-3'). The PCR product was purified, digested with NotI and BamHI, purified again, and then ligated with the NotI/BamHI-linearized pCAGGS vector. Ligation, bacterial growth, colony PCR, and sequence verification were performed using the same methods (and primers) described above for the cloning of pCAGGS-^{HA}L and pCAGGS-L^{HA}.

The plasmid expressing untagged N cloned into the pCAGGS vector (pCAGGS-N) was provided by Veronika von Messling (described in Schneider et al., 2003).

The plasmid expressing an untagged P gene (C knockout) cloned into the pCAGGS vector (pCAGGS-P) was generated by Christian Pfaller (unpublished data).

Transfection and infection assays

Transfections were performed in 293T cells with Lipofectamine 3000 and the methods described in the instructions from the manufacturer. Briefly, the plasmid DNA was mixed with Lipiofectamine 3000 and diluted in Opti-MEM. The mixture was allowed to incubate for 45

minutes with gentle mixing every 15 minutes before addition onto 293T cells. 293T cells were transfected with the individual or indicated combinations of plasmid. Amounts for each plasmid: 2 μg each of pCAGGS-N, pCAGGS-P, or pCAGGS-L, or 3 μg of pCAGGS-C^{FLAG}, pCAGGS empty vector: up to a total of 8 μg for each transfection reaction. After 4 hours of incubation at 37°C, the unsupplemented media was replaced with DMEM supplemented with 10% Fetal Bovine Serum (FBS). Alternatively, cells were infected with MeV-vac2-2tags at an MOI of 0.1 $TCID_{50}$ by allowing cells to rock for 1 hour at room temperature (RT) and then incubating at 37°C for 48 hours.

Co-immunoprecipitations assays

Cells were transfected as described above with the indicated combinations of plasmids expressing Flag-, HA-, or untagged genes or infected with MeV-vac2-2tags at an MOI of 0.1 $TCID_{50}$. At time points of 24 hours post-transfection (h.p.t.) or 48 hours post infection (h.p.i.), cells in a 35-mm dish were harvested using IP/lysis buffer (50 mM Tris, pH7.5; 150 mM NaCl; 2 mM EDTA; 1 mM Na_3VO_4; 0.5% NP-40) and freeze-thawed twice. The lysates were mixed with anti-FLAG affinity gel to pull down C^{FLAG}. After incubation at 4°C for 3 hours with rolling, the beads were collected by centrifugation and washed five times with IP/lysis buffer for 15 min each. Following addition of 25 μl of 2X urea sample buffer (200 mM Tris–HCl, pH 6.8; 8M Urea; 5% (w/v) SDS; 0.1 mM EDTA; 0.03% (w/v) Bromphenol blue; 1.4% (w/v) DTT), the samples were heated and shook at 99°C for 10 min. Samples were immediately analyzed by Western blotting.

Immunoblotting

Protein samples were resolved by SDS-8% PAGE (L-containing samples) or SDS-14% PAGE (C-containing samples), transferred onto a PVDF membrane (Millipore-Sigma), and probed with one of the following primary antibodies: anti-N505 1:5000 (Toth et al. J Virol 2009), anti-P254 1:5000 (Toth et al. J Virol 2009), anti-C2 1:5000 (Devaux et al. J Virol 2004), anti-L2170 1:1000 (unpublished), anti-FLAG M2 1:5000 (Sigma-Aldrich, St Louis, MO), or anti-HA 1:1000 (Sigma-Aldrich, St Louis, MO), followed by incubation with 1:25,000 dilution of anti-rabbit HRP or anti-mouse HRP (Jackson Immunoresearch, West Grove, PA). Blots were developed using SuperSignal West Pico Chemiluminescent substrate (Thermo Fisher, Waltham, MA) and exposed on Advansta LucentBlue x-ray film.

3.3 Results

3.3.1 Co-immunoprecipitation of C, N, and P in the presence or absence of MeV

To test whether C interacts with the MeV replication complex, we transfected 293T cells with pCAGGS expression vectors for N, P, and C^{FLAG} and tested whether N or P co-immunoprecipitated with C independent of MeV infection. We hypothesized that C interacts with one of the members of the MeV replication complex: N, P, or L. Our results showed that in the absence of MeV infection, neither N nor P supplied in isolation of other MeV proteins co-precipitated with C^{FLAG} (Figure 3.2). Alternatively, we infected 293T cells with a MeV containing a FLAG-tagged C protein and an N-terminally HA-tagged L (MeV-vac2-2tags). Based on our hypothesis that C interacts with one of the members of the MeV replication complex and prior knowledge that L interacts with P and that P interacts with N, we hypothesized that C would co-precipitate with both N and P during MeV infection. Our results

showed that in MeV-vac2-2tags infection, N, P, and the N-P complex co-precipitated with C^{FLAG}. These results indicated that C is indeed a part of the MeV replication complex, but that C requires an additional protein produced during MeV infection beyond N and P in order to associate with the complex.

3.3.2 Co-immunoprecipitation of C and L in the presence of MeV

We tested whether C^{FLAG} co-immunoprecipitated with ^{HA}L in the presence of MeV infection. Our results showed that ^{HA}L co-precipitated with C^{FLAG} during MeV infection as detected with antibodies against HA or L (Figure 3.2C,D). We attempted to test whether C^{FLAG} precipitated with ^{HA}L in the absence of MeV infection by co-transfecting the pCAGGS-C^{FLAG} construct with the pCR3-^{HA}L. However, ^{HA}L was not expressed at detectable levels in the input after multiple experimental attempts.

3.3.3 Cloning and expression of L

At slightly under 250 kDa, L is challenging to express from a plasmid vector independent of the virus due to its large size. Because our preexisting expression constructs for L (pCR3-^{HA}L and pCG-L^{HA}) did not express in our system and another preexisting expression construct for L (pCG-^{HA}L) did not reliably express in our system, we cloned two new expression constructs for L (pCAGGS-^{HA}L and pCAGGS-L^{HA}) in attempt to increase L expression. We reasoned that the pCAGGS vector may better express a large insert like full-length L due to previous experience in designing and expressing other MeV genes. Such expression construct could be used to test the interaction between C and L in the absence of other MeV proteins. pCAGGS-^{HA}L and pCAGGS-L^{HA} were cloned as described in the methods above and successfully expressed when

individually transfected into 293T cells (Figure 3.4B). Expression of pCAGGS-^{HA}L was noted in all lanes when Western blotting using HA, with highest expression detected in samples in which the cells were most confluent.

3.4 Conclusions

From our results, we concluded that C associated with L, P, and N of the MeV replication complex during MeV infection. We concluded that C did not precipitate with N or P when expressed in 293T cells in the absence of viral infection and additional methods are required to characterize the association between C and the MeV replication complex. We designed and cloned constructs of HA-tagged L and concluded that full-length L can be expressed after transfection in 293T cells. We developed a model of MeV L based on the structure of the homologous VSV L, which aided in the design of truncated L constructs. Based on our results, we propose an updated model of the MeV replication complex, in which C physically associates with the complex.

3.5 Discussion

Although the pCR3-C^{FLAG} construct successfully expressed C in our transfected cells, we cloned C^{FLAG} into the pCAGGS vector in order to normalize its expression to that of pCAGGS-N, pCAGGS-P, p-CAGGS-^{HA}L, or pCAGGS-L^{HA}. Based on previous experience, the pCAGGS vector was superior to other vectors in expressing MeV proteins in our 293T cell transfection system.

The findings that C co-precipitated with L, N, and P during MeV infection but not with N, P, or the N-P complex independent of MeV infection indicate that C physically associates with the

MeV replication complex. However, these results do not show specifically which protein or proteins associated with the MeV replication complex to which C may bind. Thus, determining the specific protein(s) in the replication complex and characterizing the C interaction site warrants further investigation. Based on the interaction of C with the replication complex during infection, we hypothesize that C interacts with one of the viral components of the replication complex, N, P, or L. Future directions of this work involve testing this hypothesis by utilizing protein complement assays to test whether a direct interaction of C with L, P, N, or combinations thereof exists and using Förster resonance energy transfer (FRET) to show the physical distance between these proteins in cells. Our results showed that that N and P did not precipitate with C when co-expressed in the absence of MeV infection (Figure 3.2). Further, preliminary experiments carried out later in 2017 indicated that C and full-length L did not co-precipitate when co-expressed in isolation of MeV (Cattaneo Lab unpublished data). The results that none of the known components of the MeV replication complex co-precipitated with C when expressed in isolation of MeV infection indicates that viral infection provides an additional factor that is not provided when proteins are expressed from transfected plasmids. For example, viral and cellular protein changes induced by other viral genes may be necessary for the interacting members of the replication complex to be in a conformation that allows for the association of C. While the transfection and co-immunoprecipitation approach provided valuable information by proving that C associates with the MeV replication complex, the approach was unable to determine the precise member with which C interacts. Nonetheless, the results of these co-immunoprecipitation experiments provided important progress in elucidating a biochemical mechanism underlying the function of C as a quality control factor in MeV replication.

The fundamental knowledge that C associates with the MeV replication complex provides an additional tool that could potentially be exploited in the rational design of modified MeV vectors for oncolytic virotherapy. It has been shown that both vaccine and wild-type MeV strains lacking C generate increased numbers of DI-RNAs, which activate innate antiviral immune response pathways, including activation of protein kinase R and interferons (Pfaller et al., 2014; Pfaller et al., 2015). Vaccine-strains MeV-Edm and MeV-vac2 are active subjects of research and development as oncolytic viruses to selectively eliminate a number of human cancers due to proven safety in humans and innate oncolytic tendencies (Msaouel et al., 2018). Thus, it is possible that future characterization of the C interaction site could serve as a target for improving the oncolytic potency of MeV. For example, one could hypothesize that residues in the interaction site could be mutated to disrupt the MeV replication complex-C interaction, decreasing the fidelity of replication and leading to the generation of additional DI-RNAs. These DI-RNAs would activate cellular stress and innate immune responses of infected cells, leading to the natural destruction of cancer cells selectively infected with the oncolytic MeV strain. Moreover, this work adds to our understanding of an important cofactor required for optimal MeV replication, which is also encoded by other closely-related viruses. Because a number of extant and emerging pathogens of humans and animals exist within the *Paramyxoviridae* family, this increased biochemical understanding of viral replication could potentially aid in the development of novel antiviral therapies.

Our investigation between MeV and C are an important step in elucidating a biochemical mechanism underlying the function of the small accessory protein C as a quality control factor in MeV replication. In a different viral system, our characterization of the relationship between the small accessory protein Ac78 and the AcMNPV sulfhydryl oxidase is a preliminary step in a

broader effort to elucidate important biochemical pathways underlying the poorly described structural changes in capsid proteins and other proteins involved in virion stability, folding, and infectivity. Taken together, the investigations of Ac78 and C and their respective relationships with the AcMNPV sulfhydryl oxidase and the MeV replication complex adds knowledge of biochemical mechanisms underlying the important functions of small accessory proteins containing less than 200 amino acids in viral replication processes of two different viral systems.

3.6 References

American Pet Product Association (AAAS). (2017). The 2017-2018 APPA National Pet Owners Survey Debut (p. 9, Rep.). Greenwich, CT: American Pet Products Association.

Audsley MD, Moseley GW. (2013). Paramyxovirus evasion of innate immunity: Diverse strategies for common targets. *J Virol.* 2(2):57-70. doi: 10.5501/wjv.v2.i2.57.

Chambers R, Takimoto T. (2009). Antagonism of innate immunity by paramyxovirus accessory proteins. *Viruses.* (3):574-93. doi: 10.3390/v1030574. Epub 2009 Oct 28.

Devoux, P., Hodge, G., McChesney, M.B., & Cattaneo, R. (2008). Attenuation of V- or C-Defective Measles Viruses: Infection Control by the Inflammatory and Interferon Responses of Rhesus Monkeys. *Molecular Therapy*, 82(11):5359. doi:10.1016/s1525-0016(16)40117-6

Griffin DE. (2013). Measles virus, p 1042–1069. In Knipe DM, Howley PM, Cohen JI, Griffin DE, Lamb RA, Martin MA, Racaniello VR, Roizman B (ed), Fields virology, 6th ed, vol 1. Lippincott Williams & Wilkins, Philadelphia, PA.

Heinemann, P., Schmidt-Chanasit, J., & Gunther, S. (2013). The N Terminus of Andes Virus L Protein Suppresses mRNA and Protein Expression in Mammalian Cells. *Journal of Virology*. 87(12), 6975-6985. doi:10.1128/jvi.00043-13

Hendriks, J., and Blume, S. (2013). Measles Vaccination Before the Measles-Mumps-Rubella Vaccine. Am J Public Health. 103(8): 1393-1401. Doi: 10.2105/AJPH.2012.301075

Hilleman, M.R. (1992). Past, present, and future of measles, mumps, and rubella virus vaccines. *Pediatrics.* 90(1 Pt 2):149-53.

Holland JJ, Kennedy SIT, Semler BL, Jones CL, Roux L, Grabau EA. (1980). Defective interfering RNA viruses and the host-cell response, p 137–192. *In* Fraenkel-Conrat H, Wagner RR. (ed), Comprehensive virology. vol 16 Plenum Press, New York, NY.

Horikami S.M. (1995). Structure, transcription, and replication of measles virus. *Curr. Top. Microbiol. Immunol.* 191:35–50.

International Committee on Taxonomy of Viruses (ICTV). (2017). Virus Taxonomy: 2013 Release, Edinburgh, Switzerland.

Ito M, Iwasaki M, Takeda M, Nakamura T, Yanagi Y, Ohno S. (2013). Measles virus nonstructural C protein modulates viral RNA polymerase activity by interacting with host protein SHCBP1. *J Virol*. 87(17):9633-42. doi: 10.1128/JVI.00714-13..

Lamb, R.A. & Parks, G.D. (2013). Paramyxoviridae, p 957–995. In Knipe DM, Howley PM, Cohen JI, Griffin DE, Lamb RA, Martin MA, Racaniello VR, Roizman B (ed). Fields virology, 6th ed, vol 1. Lippincott Williams & Wilkins, Philadelphia, PA.

Liang, B., Li, Z., Jenni, S., Rameh, A., Morin, B., Grant, T., Whelan, S. (2015). Structure of the L protein of vesicular stomatitis virus from electron cryomicroscopy. *Cell.* 162, 314-327. doi:10.2210/pdb5a22/pdb

Longhi S. (2009). Nucleocapsid structure and function. *Curr Top Microbiol Immunol* 329:103–128. doi:10.1007/978-3-540-70523-9_6

Ma, Dzwokai, et al. (2018). "Upon Infection, Cellular WD Repeat-Containing Protein 5 (WDR5) Localizes to Cytoplasmic Inclusion Bodies and Enhances Measles Virus Replication." *Journal of Virology*, vol. 92, no. 5, 2017, doi:10.1128/jvi.01726-17.

Msaouel, P., Opyrchal, M., Dispenzieri, A., Peng, K. W., Federspiel, M. J., Russell, S. J., & Galanis, E. (2018). Clinical Trials with Oncolytic Measles Virus: Current Status and Future Prospects. *Current Cancer Drug Targets,18*(2). doi:10.2174/1568009617666170222125035

Niwa H, Yamamura K, Miyazaki J. Efficient selection for high-expression transfectants with a novel eukaryotic vector. (1991). *Gene.*108(2):193-9. Epub 1991/12/15. PubMed PMID: 1660837

Parks GD, Alexander-Miller MA. (2013). Paramyxovirus activation and inhibition of innate immune responses. *J Mol Biol.* 425(24):4872-92. doi: 10.1016/j.jmb.2013.09.015.

Pfaller, C. K., Cattaneo, R., & Schnell, M. J. (2015). Reverse genetics of Mononegavirales: How they work, new vaccines, and new cancer therapeutics. *Virology.* 479-480, 331-344. doi:10.1016/j.virol.2015.01.029

Pfaller, C. K., Mastorakos, G. M., Matchett, W. E., Ma, X., Samuel, C. E., & Cattaneo, R. (2015). Measles Virus Defective Interfering RNAs Are Generated Frequently and Early in the Absence of C Protein and Can Be Destabilized by Adenosine Deaminase Acting on RNA-1-Like Hypermutations. *Journal of Virology*. 89(15), 7735-7747. doi:10.1128/jvi.01017-15

Pfaller, C. K., Radeke, M. J., Cattaneo, R., & Samuel, C. E. (2014). Measles Virus C Protein Impairs Production of Defective Copyback Double-Stranded Viral RNA and Activation of Protein Kinase R. *Journal of Virology.* 88(1), 456-468. doi:10.1128/jvi.02572-13

Radecke F, Spielhofer P, Schneider H, Kaelin K, Huber M, Dotsch C, Christiansen G, Billeter MA. (1995). Rescue of measles viruses from cloned DNA. *EMBO J.* 14:5773–5784.

Rāzī, Abū Bakr Muḥammad ibn Zakarīyā, & Greenhill, W. A. (1847). A treatise on the small-pox and measles. Birmingham, Ala.: Classics of Medicine Library.

Rima BK, Duprex WP. (2009). The measles virus replication cycle. *Curr Top Microbiol Immunol.* 329:77–102. doi:10.1007/978-3-540-70523-9_5

Sakai, K., Yoshikawa, T., Seki, F., Fukushi, S., Tahara, M., Nagata, N., . . . Takeda, M. (2013). Canine Distemper Virus Associated with a Lethal Outbreak in Monkeys Can Readily Adapt To Use Human Receptors. *J Virol.* 87(12), 7170-7175. doi:10.1128/jvi.03479-12

Schneider U, Naegele M, Staeheli P, Schwemmle M. (2003). Active borna disease virus polymerase complex requires a distinct nucleoprotein-to-phosphoprotein ratio but no viral X protein. *J Virol.* 77(21):11781-9

Van Binnendijk R.S., van der Heijden R.W. (1995). Osterhaus A.D. Monkeys in measles research. *Curr. Top. Microbiol. Immunol*. 191:135–148.

World Health Organization (WHO). (2011). Global freedom from rinderpest. 79th OIE General Session. Paris, France

World Health Organization (WHO). (2018). Measles Surveillance Data after WHO. Global summary on measles, 2006.

Zhu Y.D., Heath J., Collins J., Greene T., Antipa L., Rota P., Bellini W., McChesney M. (1997). Experimental measles. II. Infection and immunity in the rhesus macaque. *Virology*. 233:85–92. doi: 10.1006/viro.1997.8575.

3.7 Figures

Figure 3.1

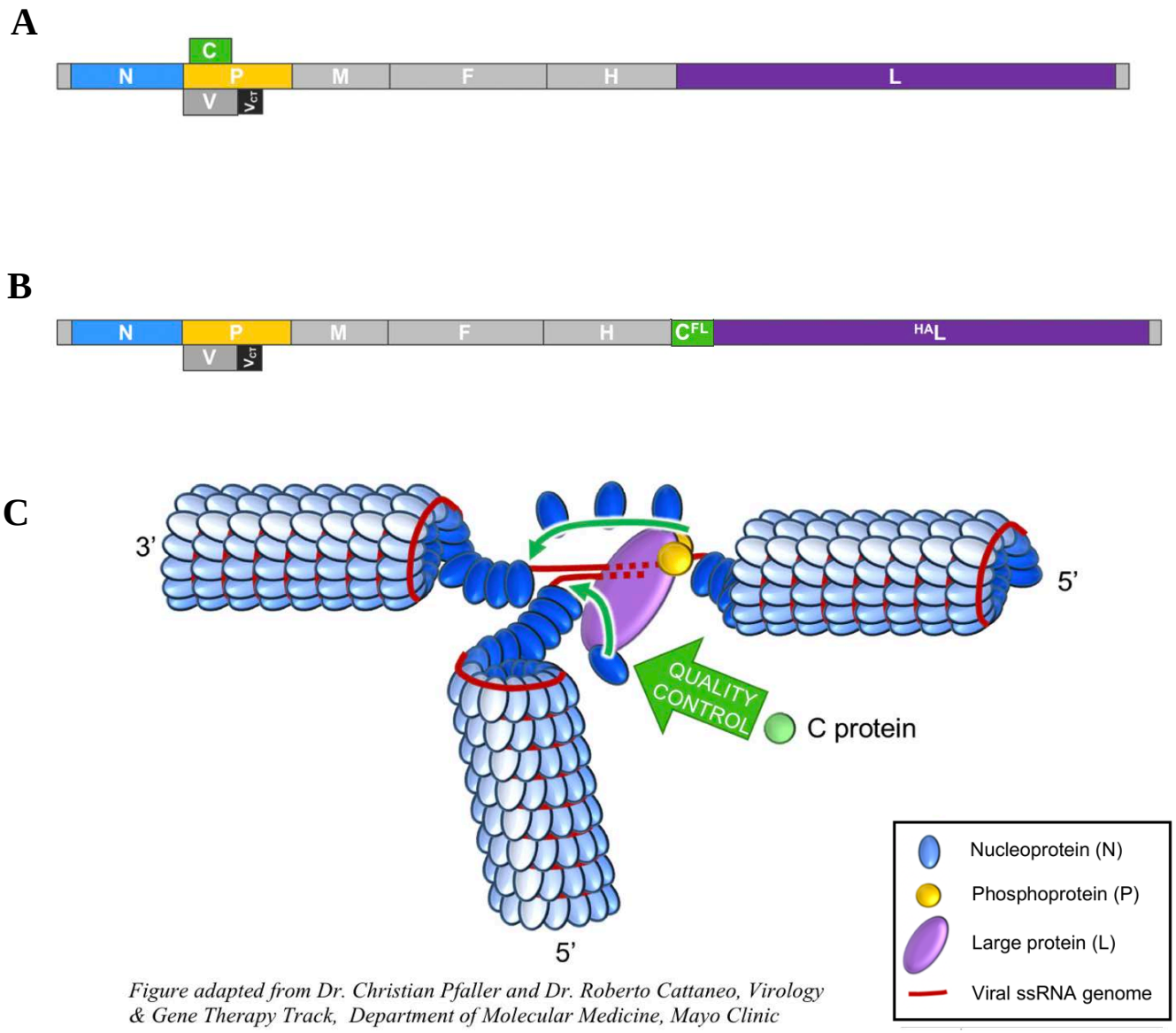

Figure adapted from Dr. Christian Pfaller and Dr. Roberto Cattaneo, Virology & Gene Therapy Track, Department of Molecular Medicine, Mayo Clinic

Figure 3.1 - MeV genome organization and schematic representation of the viral replication complex

(A) Schematic representation of the MeV genome. In the standard MeV, C protein is expressed from the P/V/C gene.

(B) Our modified virus MeV-vac2-2tags expresses both a FLAG-tagged C (C^{FLAG}) from an additional gene between H and L genes and an HA-tagged L protein (^{HA}L). The endogenous C was deleted from this virus.

(C) The MeV ssRNA genome is encapsidated by N. L and P form the viral RNA-dependent RNA polymerase, which extracts the RNA molecule from the nucleocapsid stepwise during synthesis. P walks the polymerase along the nucleocapsid lattice, while L confers all catalytic functions. The template and nascent ssRNA strands are immediately separated and encapsidated with N. Additionally depicted is our preexisting hypothesis that C physically associates with this replication complex and serves as an important quality control factor.

Figure 3.2

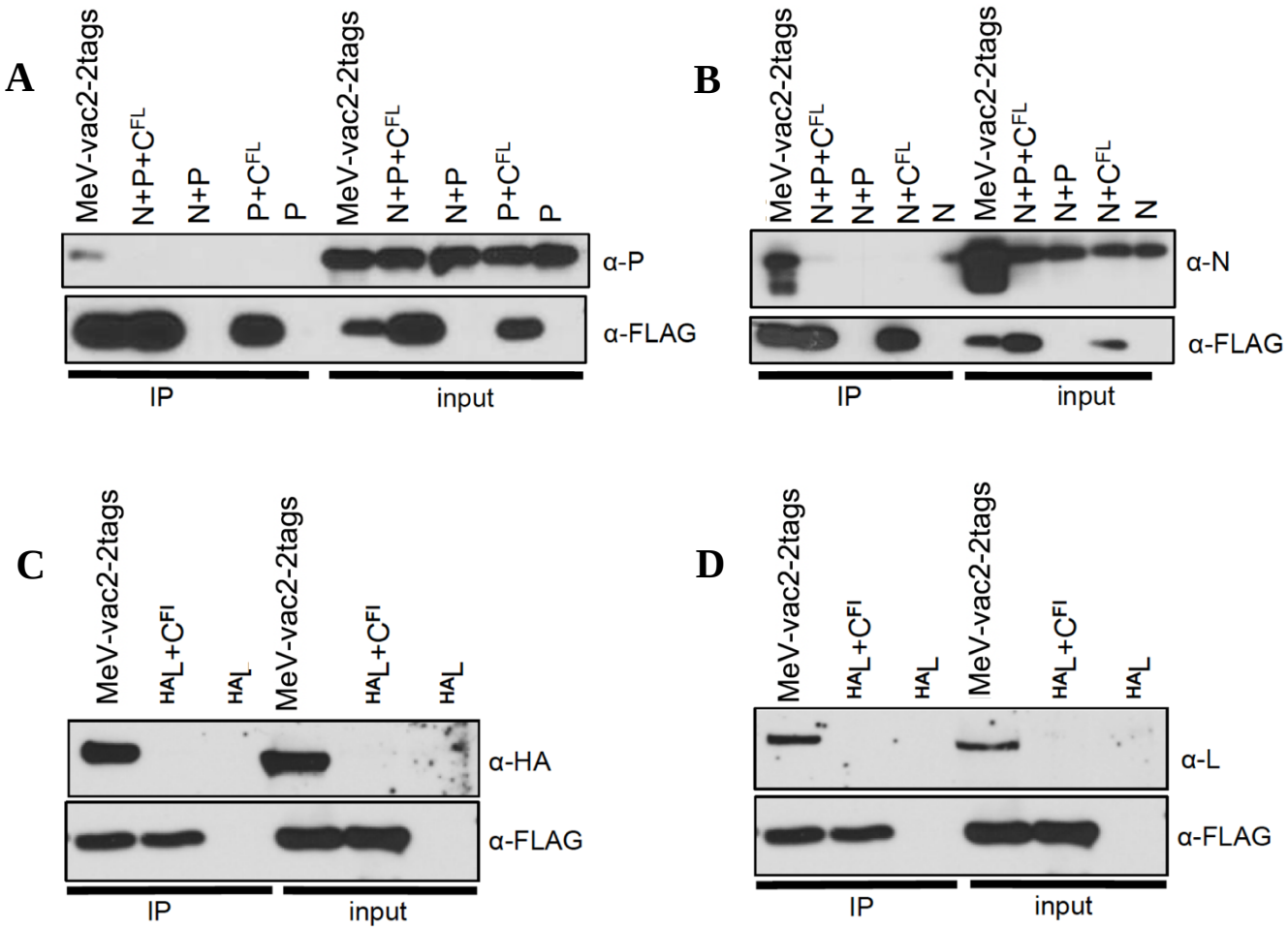
A
MeV-vac2-2tags
N+P+C^FL
N+P
P+C^FL
P
MeV-vac2-2tags
N+P+C^FL
N+P
P+C^FL
P
α-P
α-FLAG
IP
input
B
MeV-vac2-2tags
N+P+C^FL
N+P
N+C^FL
N
MeV-vac2-2tags
N+P+C^FL
N+P
N+C^FL
N
α-N
α-FLAG
IP
input
C
MeV-vac2-2tags
HAL+C^FI
HAL
MeV-vac2-2tags
HAL+C^FI
HAL
α-HA
α-FLAG
IP
input
D
MeV-vac2-2tags
HAL+C^FI
HAL
MeV-vac2-2tags
HAL+C^FI
HAL
α-L
α-FLAG
IP
input

Figure 3.2: C co-immunoprecipitated with L, N, and P during MeV infection but did not associate with N, P, or the N+P complex in the absence of MeV infection

(A) C co-immunoprecipitated with P in the presence of MeV infection but did not co-immunoprecipitate with P or the N+P complex in the absence of MeV infection. Western blot analysis of lysates from 293T cells infected with MeV-vac2-2tags or transfected with the indicated combinations of expression vectors for N, P, and C^{FLAG}. C^{FLAG} was precipitated using anti-FLAG affinity gel. An antibody raised against full-length P was used for detection in Western Blot analysis.

(B) C co-immunoprecipitated with N in the presence of MeV infection but did not co-immunoprecipitate with N or the N+P complex in the absence of MeV infection. An antibody raised against full-length N was used for detection in Western Blot analysis.

(C & D) C co-immunoprecipitated with L in the presence of MeV infection. Lysates from 293T cells infected with MeV-vac2-2tags or transfected with ^{HA}L (pCR3-^{HA}L) or $^{HA}L+C^{FLAG}$ plasmids. CFLAG was precipitated using anti-FLAG affinity gel. C was detected using an anti-FLAG antibody, and L was detected using anti-HA antibody (C) or anti-L antibody (D).

Figure 3.3

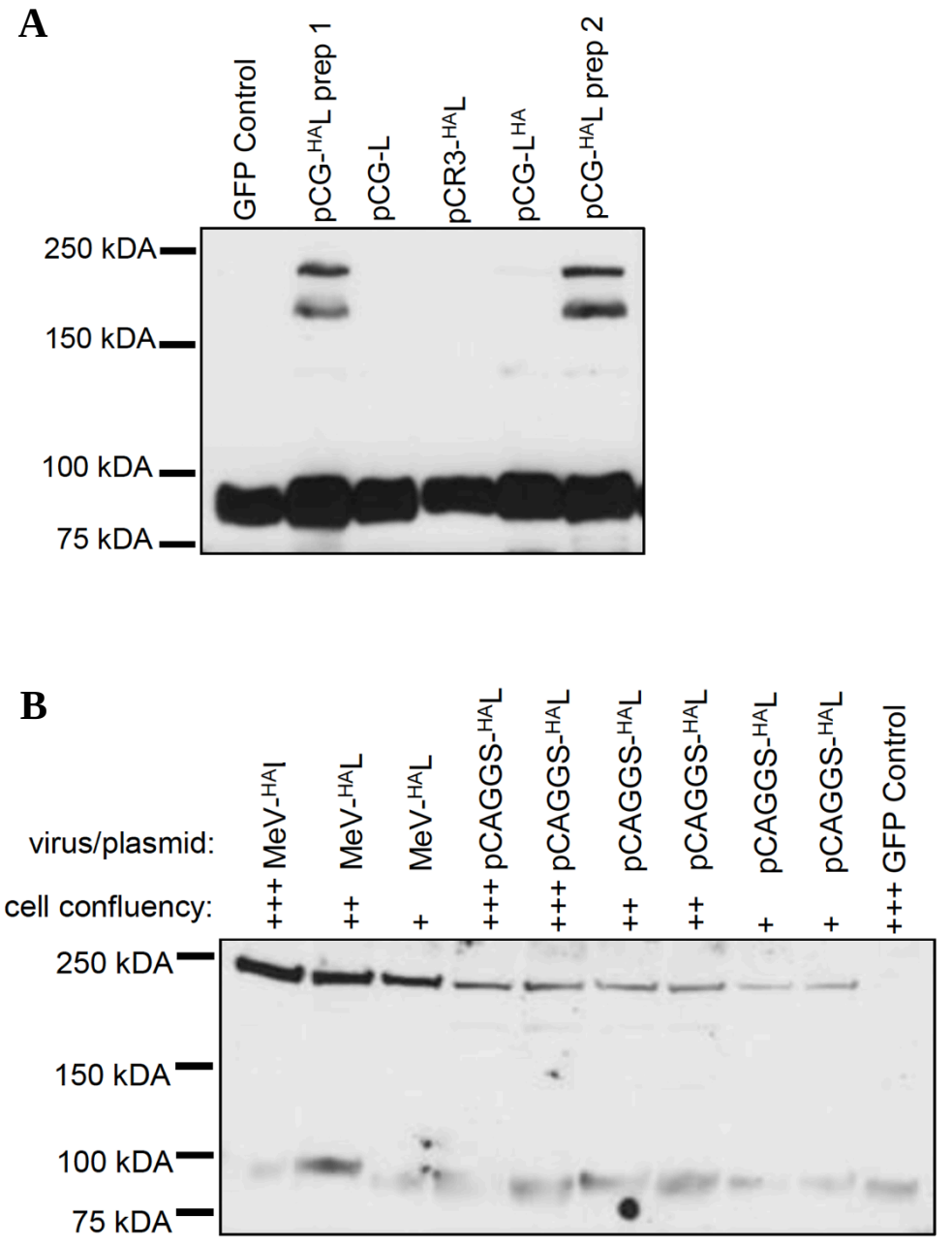
A
GFP Control
pCG-HAL prep 1
pCG-L
pCR3-HAL
pCG-LHA
pCG-HAL prep 2
250 kDA
150 kDA
100 kDA
75 kDA
B
virus/plasmid:
cell confluency:
+++ MeV-HAI
++ MeV-HAL
+ MeV-HAL
+++ pCAGGS-HAL
+++ pCAGGS-HAL
++ pCAGGS-HAL
++ pCAGGS-HAL
+ pCAGGS-HAL
+ pCAGGS-HAL
+++ GFP Control
250 kDA
150 kDA
100 kDA
75 kDA

Figure 3.3 - L can be transiently expressed via transfection of 293T cells

(A) Lysates from 293T cells transfected with different plasmid constructs of HA-tagged L cloned into the pCG or pCR3 vectors and detected by Western blotting and anti-HA. Two L-specific bands were detected in pCG-^{HA}L: one band at the expected size for L of slightly smaller than 250 kDa and one band slightly larger than 150 kDa. Non-specific bands were present just below 100 kDa. No L was expressed from pCR3 vector.

(B) Lysates from 293T cells infected with MeV-vac2-2tags or transfected with HA-tagged L cloned into the pCAGGS vector. Expression of pCAGGS-^{HA}L was noted in all lanes, with highest expression occurring in samples in which the cells were most confluent. Detected with anti-HA.